JGR Biogeosciences

RESEARCH ARTICLE
10.1029/2022JG006932

Mixed Signals From the Stable Isotope Composition of Precipitation and Plant Waxes in the Northern Tropical Andes

Lina C. Pérez-Angel[1,2,3,4], Julio Sepúlveda[1,2], Camilo Montes[5], Jamila J. Smith[6], Peter Molnar[1,3,†], Catalina González-Arango[7], Kathryn E. Snell[1], and Nadia Dildar[2]

[1]Department of Geological Sciences, University of Colorado Boulder, Boulder, CO, USA, [2]Institute of Arctic and Alpine Research (INSTAAR), University of Colorado Boulder, Boulder, CO, USA, [3]Cooperative Institute for Research in Environmental Sciences, University of Colorado Boulder, Boulder, CO, USA, [4]Institute at Brown for Environment and Society, Department of Earth, Environment and Planetary Sciences, Brown University, Providence, RI, USA, [5]Department of Physics and Geosciences, Universidad del Norte, Barranquilla, Colombia, [6]Geology and Environmental Sciences Department, Fredonia State University of New York, Fredonia, NY, USA, [7]Department of Biological Sciences, Universidad de Los Andes, Bogotá, Colombia

Abstract We evaluate the efficacy of the stable isotope composition of precipitation and plant waxes as proxies for paleoaltimetry and paleohydrology in the northern tropical Andes. We report monthly hydrogen (δ^2H_p) and oxygen ($\delta^{18}O_p$) isotope values of precipitation for an annual cycle, and hydrogen isotope values of plant waxes (δ^2H_{wax}) obtained from modern soils along the eastern and western flanks of the Eastern Cordillera of Colombia. δ^2H_p, $\delta^{18}O_p$, as well as the unweighted mean δ^2H_{wax} values of *n*-C_{29}, *n*-C_{31}, and *n*-C_{33} *n*-alkanes in the eastern flank show a dependence on elevation ($R^2 = 0.90$, 0.82, and 0.65, respectively). In stark contrast, the stable isotope compositions of neither precipitation nor plant waxes from the western flank correlate with elevation ($R^2 < 0.23$), on top of a negligible (p-value >0.05) correlation between δ^2H_{wax} and δ^2H_p. In general, δ^2H_{wax} values along the eastern flank of the Eastern Cordillera seem to follow the trend of a simple Rayleigh distillation process that is consistent with studies elsewhere on the eastern side of the Andes in South America. Neither δ^2H_p nor $\delta^{18}O_p$, and therefore δ^2H_{wax}, offer reliable estimates of past elevations in the western flank, due perhaps to water vapor source mixing, evaporation overprint, contrasting plant communities, and/or differences in evapotranspiration. Thus, δ^2H_{wax} is only reliable for paleohydrology and paleoaltimetry reconstructions on the eastern flank of the Andes, whereas interpretations based on δ^2H_p and/or $\delta^{18}O_p$ west of the highest point of the Eastern Cordillera need to consider mixing of moisture sources in addition to precipitation amount.

Plain Language Summary As air rises over mountainous terrain, heavy isotopes of hydrogen and oxygen preferentially enter the condensate and rain out during ascent leaving remaining vapor depleted in the heavy isotopes. Previous studies have shown that stable isotope values of both precipitation and plant waxes correlate with elevation, and therefore, can be used to reconstruct past surface elevations. This correlation with elevation is clear on the eastern flank of the Eastern Cordillera of Colombia in the northern tropical Andes. On the western flank, however, no correlation was found for either precipitation or plant waxes. Complex atmospheric circulation and the topographic configuration of inter-Andean valleys pose a challenge for simple isotope signals. It follows that geologists carrying out paleoaltimetry and paleohydrology studies using stable isotopes should be wary of mixed moisture sources and/or complex evaporation paths and be more confident in paleoelevation and paleoclimate estimates if moisture sources are simple.

1. Introduction

The dependence of the stable isotope composition of meteoric waters on elevation has been used as a tool in paleoaltimetry to reconstruct past surface elevations (e.g., Blisniuk & Stern, 2005; Garzione, Dettman, et al., 2000, Garzione, Quade, et al., 2000; Jackson et al., 2019; Li & Garzione, 2017; Mulch et al., 2008; Rowley et al., 2001). The hydrogen (δ^2H_p) and oxygen ($\delta^{18}O_p$) isotope values of precipitation decrease with elevation as moist air rises over high terrain, cools, and condenses; this is one of the results of a process known as Rayleigh distillation (Garelick et al., 2021; Rowley, 2007, 2018; Rowley et al., 2001; Rowley & Garzione, 2007). Thus, the preservation of ancient stable isotope compositions of water in the rock record, as recorded in climate proxies, can be used to reconstruct changes in surface elevation over time.

Key Points:

- The stable isotope composition of precipitation and plant waxes in the eastern flank of the Eastern Cordillera record an elevation-dependent signal
- The stable isotope composition of neither precipitation nor plant waxes from the western flank correlate with elevation
- Stable isotopes are unreliable paleoaltimeters when multiple water vapor sources and/or evaporation overprint simple Rayleigh distillation

Supporting Information:

Supporting Information may be found in the online version of this article.

Correspondence to:

L. C. Pérez-Angel,
lina.perezangel@colorado.edu;
lina_perez_angel@brown.edu

Citation:

Pérez-Angel, L. C., Sepúlveda, J., Montes, C., Smith, J. J., Molnar, P., González-Arango, C., et al. (2022). Mixed signals from the stable isotope composition of precipitation and plant waxes in the northern tropical Andes. *Journal of Geophysical Research: Biogeosciences*, *127*, e2022JG006932. https://doi.org/10.1029/2022JG006932

Received 15 APR 2022
Accepted 23 NOV 2022

Author Contributions:

Conceptualization: Lina C. Pérez-Angel, Julio Sepúlveda, Camilo Montes, Peter Molnar
Data curation: Jamila J. Smith, Nadia Dildar
Formal analysis: Lina C. Pérez-Angel, Jamila J. Smith, Nadia Dildar
Funding acquisition: Lina C. Pérez-Angel, Julio Sepúlveda, Peter Molnar, Kathryn E. Snell
Investigation: Lina C. Pérez-Angel, Camilo Montes, Jamila J. Smith, Peter Molnar
Methodology: Lina C. Pérez-Angel, Julio Sepúlveda, Jamila J. Smith

Project Administration: Lina C. Pérez-Angel, Julio Sepúlveda, Peter Molnar
Resources: Lina C. Pérez-Angel, Julio Sepúlveda, Camilo Montes
Software: Lina C. Pérez-Angel, Jamila J. Smith, Nadia Dildar
Supervision: Julio Sepúlveda, Camilo Montes, Peter Molnar, Catalina González-Arango, Kathryn E. Snell
Validation: Lina C. Pérez-Angel, Peter Molnar
Visualization: Lina C. Pérez-Angel, Camilo Montes
Writing – original draft: Lina C. Pérez-Angel
Writing – review & editing: Lina C. Pérez-Angel, Julio Sepúlveda, Camilo Montes, Peter Molnar, Catalina González-Arango, Kathryn E. Snell, Nadia Dildar

The hydrogen isotope composition of plant waxes (δ^2H_{wax}) preserved in sedimentary archives has emerged as an important proxy to study δ^2H_p in the past (Eglinton & Eglinton, 2008; Sachse et al., 2006, 2012; Sauer et al., 2001). Plant waxes are ubiquitous *n*-alkyl lipids in nature produced by terrestrial and aquatic plants (Diefendorf & Freimuth, 2017; Eglinton & Hamilton, 1967; Freimuth et al., 2017) that incorporate the isotopic composition of environmental water into their chemical structures (Sachse et al., 2006, 2012), and that can be preserved in sedimentary records for hundreds of millions of years. Consequently, δ^2H_{wax} values from sedimentary archives have been used as a paleohydrological proxy in the geologic record (Garelick et al., 2021; Pagani et al., 2006; Polissar et al., 2009; Schefuβ et al., 2005; Super et al., 2018; Tierney et al., 2008; Williford et al., 2014). Modern studies using plants and soils along elevation transects (i.e., Tibetan Plateau, China, Central and South-Central Andes, Ethiopia, and the Pamirs) have shown that δ^2H_{wax} values can capture the effects of a topographic barrier on the stable isotope composition of precipitation, and thus, when preserved in sedimentary archives, can be used to reconstruct past precipitation associated with elevation (Aichner et al., 2021; Bai et al., 2011; Feakins et al., 2018; Jaeschke et al., 2018; Luo et al., 2011; Nieto-Moreno et al., 2016; Ponton et al., 2014). Several studies have attempted to use such proxies to reconstruct past elevations in the rock record in places like the Tibetan Plateau (Polissar et al., 2009), the Sierra Nevada in the western United States (Hren et al., 2010), the northern Altiplano in Perú (Kar et al., 2016), and the Eastern Cordillera of Colombia (Anderson et al., 2015).

A mountain region that remains elusive regarding its paleoaltimetry history is the Sabana de Bogotá in the Eastern Cordillera of Colombia. Previous studies using pollen records and thermochronology in the region led to the inference that surface uplift happened since ∼6 – 3 Ma (e.g., Helmens & Van der Hammen, 1994; Hooghiemstra et al., 2006; Hooghiemstra & Van Der Hammen, 1998; Mora et al., 2008; Van der Hammen et al., 1973; Wijninga, 1996; Wijninga & Kuhry, 1990). Both the timing and tectonic processes of this surface uplift have been challenged by other authors using different proxies or alternative climate-based explanations (Anderson, 1972; Anderson et al., 2015; Bayona et al., 2008; Molnar & Pérez-Angel, 2021; Mora-Páez et al., 2016; Pérez-Angel & Molnar, 2017). Saylor et al. (2009) showed that δ^2H and $\delta^{18}O$ values of modern surface waters in the eastern flank of the Eastern Cordillera of Colombia record a dependence on altitude, suggesting its utility as a paleoaltimetry proxy. A previous study using the δ^2H_{wax} values of *n*-alkanes from sedimentary archives in the Sabana de Bogotá (Anderson et al., 2015), however, showed no systematic trend in surface uplift over the past ∼7 Ma. The latter contradicted the authors' inferences of ∼1,000 m of surface uplift during this time using temperature reconstructions based on bacterial lipids. Thus, a better understanding of the modern regional processes controlling the isotopic composition of precipitation and plant waxes preserved in soils could allow us to improve precipitation reconstructions and their paleoclimate and paleoelevation implications.

We evaluate the regional and temporal configuration of precipitation patterns, as well as the stable isotope composition of precipitation and sedimentary plant waxes along two altitudinal transects in the Eastern Cordillera of Colombia. Our study includes results across the eastern flank, which is the first east-to-west topographic barrier encountered by moisture from the Amazon basin, and the western flank, whose base lies in an inter-Andean valley. We present results on the δ^2H_p and $\delta^{18}O_p$ values of 176 samples of monthly precipitation over a year cycle, and the δ^2H_{wax} values of long-chain plant wax *n*-alkanes (*n*-C_{29}, *n*-C_{31}, and *n*-C_{33}) preserved in top soils at 16 sites (Figure 1). We then used this data to disentangle the interrelationships among elevation, precipitation amount, sources of precipitation, and vapor pressure deficit (VPD) influencing δ^2H_{wax} values. Finally, we evaluated the utility of δ^2H_{wax} as an altitudinal and hydrological proxy in the region.

2. Background

2.1. Hydroclimate of Northwest South America

The annual hydrological cycle of northern tropical South America is controlled mainly by the meridional migration of the Intertropical Convergence Zone (ITCZ; Alvarez-Villa et al. [2011]; Espinoza et al. [2009, 2020]; Mejia et al. [1999]; Poveda et al. [2001]; Sierra et al. [2015]). In Colombia, where the tropical Andes is divided into three cordilleras (Figure 1a), the precipitation seasonality can vary across geographic and topographic features. Precipitation in the Western and Central Cordilleras consists mostly of a bimodal annual cycle with the two rainy seasons in March–April–May and September–October–November (Bendix & Lauer, 1992; Espinoza et al., 2020; Mejia et al., 1999; Ricaurte et al., 2019). By contrast, in the eastern foothills of the eastern side of the Andes, in the tropical lowlands, and in the Caribbean region, a unimodal annual cycle of precipitation occurs (Espinoza et al., 2020; Urrea et al., 2019). For the eastern slope of the Colombian Andes, the maximum precipitation occurs

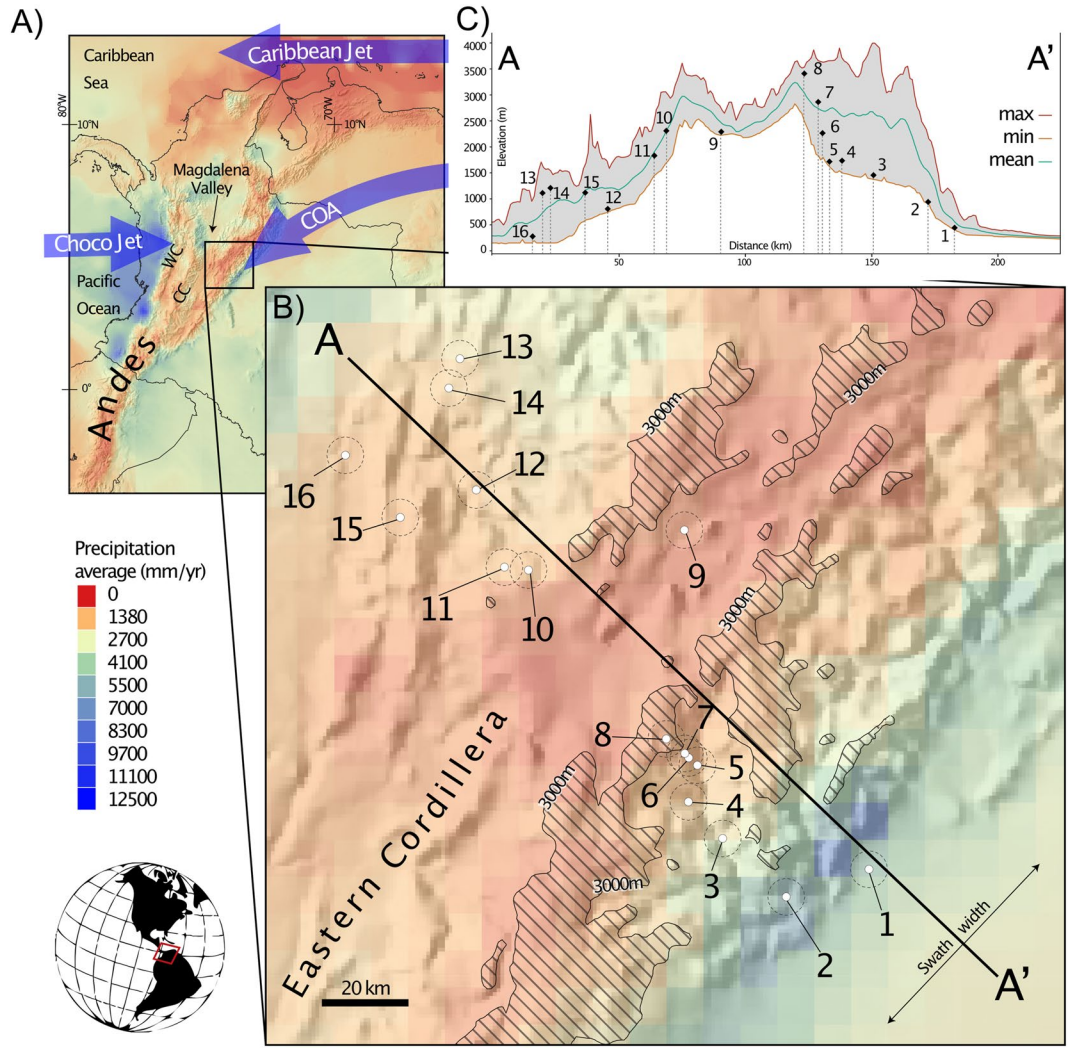

Figure 1. (a) Topographic map of northwest South America showing annual rainfall based on Hurtado-Montoya and Mesa-Sánchez (2014); WC and CC show the Western Cordillera and the Central Cordillera of Colombia, respectively. The Magdalena Valley is shown between the Central Cordillera and the Eastern Cordillera. Arrows represent paths of moisture transport of the three low level jets that affect annual variability of precipitation in Colombia: Caribbean Low-Level Jet, Choco Jet, and Corriente de los Andes Orientales (CAO). (b) Close up of the study area in the Eastern Cordillera of Colombia. Sites 1–8 show the eastern flank altitudinal transect and sites 9–16 show the western flank altitudinal transect. (c) The A to A' swath profile shows the topographic cross section of the transects with maximum (max), minimum (min) and mean elevations.

during June-July-August, when the westward advection of moisture from the Amazon encounters the Eastern Cordillera as a topographic barrier (Poveda et al., 2006). In the Caribbean region, the unimodal cycle is not only influenced by the ITCZ, but also by incursions from the easterly Caribbean low-level jet (Arias et al., 2015; Poveda et al., 2006).

The meridional migration of the ITCZ in the northern tropical Andes is intertwined with other features of the atmospheric circulation and with different water vapor sources from the Caribbean Sea, the eastern Pacific Ocean, and the Atlantic/Amazon basin (Arias et al., 2021; Bedoya-Soto et al., 2019; Espinoza et al., 2020; Hoyos et al., 2018; Poveda et al., 2006; Poveda & Mesa, 2000; Sierra et al., 2021; Urrea et al., 2019). These atmospheric features are low-level jets that influence the annual variability of precipitation: the Choco jet, the Caribbean jet, and the Corriente de los Andes Orientales (CAO) or the Orinoco jet (Figure 1a). The complexity of the topography in the region, in addition to the different sources of moisture and differing winds, create dynamic precipitation patterns in the northern tropical Andes of Colombia.

2.2. Stable Isotope Composition of Precipitation in Colombia

Rodríguez (2004) suggested that the dominant control on the stable isotope composition of precipitation in Colombia is the amount effect, which is the correlation of the amount of rain that falls with the extent of ^{18}O- and ^{2}H-depletion of the rainfall. The amount effect in Colombia is marked by the seasonality between dry and wet months, which is spatially variable within the region. In addition to seasonality, Rodríguez (2004) suggested that the source of water vapor that precipitates over the Eastern Cordillera (Figure 1) differs from that in the Central Cordillera and to the west. He based that inference on differing regressions of $\delta^{2}H_{p}$ values against $\delta^{18}O_{p}$ values; that is, the $\delta^{18}O_{p}$ intercept for a station in the Central Cordillera is 10‰, whereas for a station in the Eastern Cordillera it is 9‰. Additionally, Rodríguez (2004) compared the variability of the stable isotope composition of precipitation between the interior of the continent (Eastern Cordillera) and near the Caribbean Sea and concluded that the highest variability is in the former. Later, Saylor et al. (2009) analyzed spatial and temporal variations in the stable isotope composition of surface waters with topography across the flanks of the Eastern Cordillera of Colombia. After excluding sites near the Magdalena valley, these authors concluded that the eastern side of the Eastern Cordillera closely follows a one-dimensional Rayleigh distillation model, and suggested that the stable isotope composition of meteoric water could be used for paleoelevation estimates in this region.

2.3. Stable Isotope Composition of Plant Waxes: Paleohydrology and Paleoaltimetry

Plant waxes are *n*-alkyl lipids (*n*-alkanes, *n*-alcohols, *n*-alkanoic acids, and wax esters) produced by terrestrial and aquatic plants (Diefendorf & Freimuth, 2017; Eglinton & Hamilton, 1967). The hydrogen ($\delta^{2}H_{wax}$) and carbon ($\delta^{13}C_{wax}$) isotope compositions of plant waxes can reflect the physical, chemical, biological, and ecological conditions of the environment in which they grow, such as the precipitation/evaporation balance (hydrological cycle), temperature, and the composition of the plant community (i.e., C_3 and C_4 plants; Diefendorf & Freimuth, 2017). Terrestrial plants, which produce predominantly long-chain waxes, incorporate and fractionate the hydrogen isotope composition of the source water (Goldsmith et al., 2019; Ladd et al., 2021; McFarlin et al., 2019; Sachse et al., 2012). The main source of water for terrestrial plants is soil moisture, which in turn derives its original isotopic composition from the local precipitation. Because precipitation varies in time and space, the stable isotope composition of such source water records the amount-weighted mean of precipitation rates (Sachse et al., 2012). Several calibration studies have shown a baseline for interpretations of the variability of $\delta^{2}H_{wax}$ values, making it a valuable proxy for reconstructing hydroclimate through time (Chikaraishi & Naraoka, 2003; Feakins & Sessions, 2010; Hou et al., 2008; Krull et al., 2006; Smith & Freeman, 2006). Further studies have shown that $\delta^{2}H_{wax}$ can also track the altitude effect of precipitation (Bai et al., 2011; Feakins et al., 2016; Wang et al., 2017), and when preserved in soils and sediment, they can be used as a proxy to reconstruct past surface elevations (e.g., Feakins et al., 2018; Nieto-Moreno et al., 2016; Polissar et al., 2009). In the Central (Ponton et al., 2014) and South Central (Nieto-Moreno et al., 2016) Andes, $\delta^{2}H_{wax}$ values of soil-derived *n*-alkanes match the modern elevation-dependence of precipitation. These altitudinal transects, however, cross the eastern slope of the Andes, where the isotopic composition of water vapor in the atmosphere follows a simple Rayleigh distillation process when encountering the topographic barrier of the Andes from the Amazon.

3. Methods

3.1. Study Area and Sample Collection

We collected 16 top soil samples (5–10 cm depth) at 16 sites along two altitudinal transects in the Eastern Cordillera of Colombia as reported by Pérez-Angel et al. (2020) (Figure 1). The eastern flank transect spanned ∼3,000 m of elevation, from Los Llanos (4.266°N, 73.543°W, 423 m, site 1) to the Páramo El Verjón (4.560°N, 74.000°W, 3,359 m, site 8), whereas the transect across the western flank spanned ∼2,000 m of elevation, from Honda in the Magdalena valley (5.200°N, 74.724°W, 218 m, site 16) to Zipaquirá in the western side of the Sabana de Bogotá (5.032°N, 73.960°W, 2,589 m, site 9) (Figure 1). In addition to soils, we also collected monthly precipitation samples for stable isotope analysis for a full annual cycle between August 2017 and September 2018. We recovered all precipitation samples except for station 10 in the western flank (Figure 1).

3.2. Precipitation Amount and Stable Isotope Analysis

To obtain precipitation amount values for each of the stations with isotopic data, we interrogated the database of Hurtado-Montoya and Mesa-Sánchez (2014). This database contains the monthly precipitation amounts in Colombia derived from a reanalysis of rain gauges and satellite data for the 1975–2006 period with a 5 min-resolution (0.0833°) in both latitude and longitude (~9.3 km per pixel). Because of the steep topographic gradients in the eastern flank of the Eastern Cordillera of Colombia and the short horizontal distances between some stations, three stations with more than ~1,000 m elevation difference fall on the same pixel grid with the same precipitation pixel value. To avoid this artifact, we instead interrogated the average precipitation raster for the 1975–2006 interval using a 0.04165° (~4.6 km) radius buffer around each station (dotted circles around each station in Figure 1b). Thus, the precipitation amount for each station is the result of the zonal mean of the yearly precipitation amount value, with a size comparable to the original 5 min-resolution precipitation amount data from Hurtado-Montoya and Mesa-Sánchez (2014). We then used precipitation amount values to calculate the annual weighted arithmetic mean for the stable isotope composition of precipitation at each site (Table S2 in Data Set S1).

We analyzed a total of 176 monthly precipitation samples in the Stable Isotope Laboratory at the Institute of Arctic and Alpine Research at the University of Colorado Boulder (Table S1 in Data Set S1). The δ^2H_p and $\delta^{18}O_p$ values were obtained using a Picarro L2130-i Cavity Ring-Down Mass Spectrometer. Each sample was run 6 times, and only the last three values were considered for the mean value. For every 20 samples, a replicate was run to check for reproducibility. We report data using δ notation in per mil (‰) relative to VSMOW. We analyzed multiple sets of secondary water standards calibrated to VSMOW2 and SLAP in between samples. Analytical error for the δ^2H_p and $\delta^{18}O_p$ values was 1‰ and 0.1‰, respectively.

We calculated the mean annual δ^2H_p and $\delta^{18}O_p$ values for each station, and we made sure that each site had 12 data points. For seven time points in a total of four stations (9, 12, 13, and 16; Figure 1), no data was obtained because of a lack of precipitation. A total of six samples from stations 1, 2, 4, 5, 15, and 16 were lost or compromised by evaporation during transport from the field to the laboratory. For these stations, we interpolated missing values by obtaining a mean value between the preceding and subsequent months. We then used monthly precipitation amounts for each station to obtain a weighted mean annual stable isotope composition. Because our study only covers one year of data, we used the Bogotá (4.7°N, 74.13°W, 2,547 m) Global Network of Isotopes in Precipitation (GNIP) station to estimate the monthly and annual δ^2H_p and $\delta^{18}O_p$ means, the 1-sigma (1σ) annual variability, and their corresponding precipitation amount. The calculated variability was then assigned as the uncertainty for annual mean δ^2H_p and $\delta^{18}O_p$ values of precipitation at each station. To avoid biasing annual averages towards months with more data samples than others, we chose a total of 10 years with 12 consecutive months of data (Table S1 in Supporting Information S1).

3.3. Extraction and Analysis of Plant Wax *n*-Alkanes

Soil samples were freeze dried, homogenized, and sieved (0.3 mm mesh) to remove plant debris, roots, and coarse particles as detailed in Pérez-Angel et al. (2020). We extracted total lipid extracts (TLEs) out of ~8 g of soil for each sample with dichloromethane:methanol (DCM:MeOH 9:1 v:v) using an accelerated solvent extractor (DIONEX ASE 200; 100°C and 2,000 psi). We evaporated TLEs at 30°C under a gentle N_2 stream using a Turbovap. We then removed elemental sulfur using copper pellets previously activated with HCL for at least 1 hr. We spiked samples with 1,000 ng 3-methyl heneicosane as an internal standard. Later, we filtered the TLEs through a short Pasteur pipette filled with glass wool and sand:Na_2SO_4 (8:2) to remove any particles and water, and evaporated them once again to determine their mass. Finally, we separated TLEs into 5 lipid classes by liquid chromatography using short Pasteur pipettes filled with silica gel. Aliphatic hydrocarbons, aromatic hydrocarbons, ketones, alcohols, and acids were eluted with hexane (3/4 dead volume, DV), hexane:dichloromethane 4:1 (Hexane:DCM; 2 DV), dichloromethane (DCM; 2 DV), dichloromethane:ethyl acetate 1:1 (DCM:EtOAc; 2DV), and ethyl acetate (EtOAc, 2 DV), respectively. Aliphatic hydrocarbons were then evaporated under a gentle nitrogen stream and transferred into 2 mL vials with glass inserts before analysis.

n-Alkanes were analyzed in full-scan mode (50–600 m/z) using a Thermo Trace 1310 Gas Chromatograph coupled to a TSQ Evo 8000 triple quadrupole mass spectrometer (GC-QQQ-MS). We used a DB-1MS GC column (60 m, 0.25 mm I.D., 0.25 µm film thickness; Agilent Technologies). The PTV injector was equipped

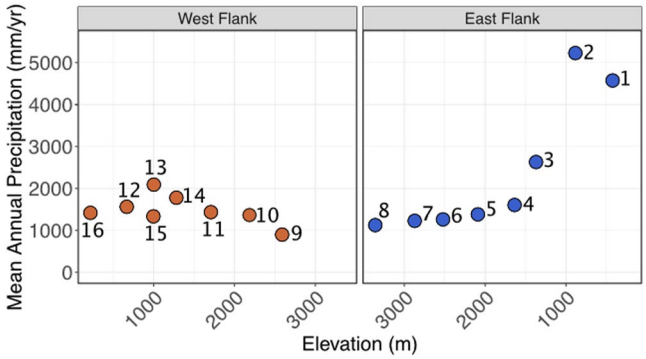

Figure 2. Mean annual precipitation (mm/yr) for each site versus elevation for each flank of the Eastern cordillera. Site numbers are identical to those in Figure 1.

with a baffled glass liner, operated in splitless mode, and the temperature ramped from 60°C to 300°C at a rate of 14.5°C/s. The GC oven temperature program was: 60°C (hold for 2 min) to 220°C at 15°C/min, to 315°C at 3°C/min, and then held at 315°C for 30 min. Long-chain *n*-alkanes (C_{27}-C_{35}) were quantified using the response factor of the 3-methyl heneicosane internal standard.

3.4. Compound Specific δ^2H in *n*-Alkanes

δ^2H_{wax} values were measured by gas chromatography - isotope ratio mass spectrometry (GC-IRMS) using a Thermo Scientific 253 Plus equipped with universal CNOS and HD collectors, a Conflo IV interface, a GC Isolink II, and a Trace GC 1310. The pyrolysis reactor was set at 1420°C. The GC column and oven method were identical to the GC-MS conditions described in Section 3.3. We used the A6 *n*-alkane standard mix (Arndt Schimmelmann) for linearity correction and isotopic calibration. The root-mean-square deviation (RMSD) was <5‰ and the H_3^+ factor remained consistent around 10. Additionally, we checked instrument performance by monitoring a non-isotopic co-injection standard (150 ng of 5α-cholestane). All samples were run at least in duplicate, and sometimes in triplicate, and data were processed using the Isoverse R packages (Isoreader: Kopf et al. [2021]; Isoprocessor: www.isoverse.org/packages/). We only used signal intensities above 4V of amplitude (Supplementary Information S2), and we report the isotopic composition of individual compounds as the average of up to three replicates (Table S3 in Data Set S1).

We calculated the apparent fractionation between precipitation and plant waxes using the following equation:

$$\varepsilon_{wax/p} = 1000 \times \left(\frac{\delta^2H_{wax} + 1000}{\delta^2H_p + 1000} \right) - 1 \quad (1)$$

4. Results

4.1. Amount and Stable Isotope Composition of Precipitation

On an annual basis, the eastern foothills of the Eastern Cordillera receive twice as much rain as its western flank and the high elevation sites of the eastern flank (Figure 2). Monthly precipitation amounts at our study sites show the expected bimodal seasonality in precipitation along the western flank compared to the unimodal seasonality of the eastern flank (bar plots, Figure 3). On average, the months with the least precipitation amount on the western flank are December–January–February (~68–104 mm/month) and June–July–August (~71–76 mm/month). Unlike the western flank, precipitation amounts on the eastern flank during June-July-August are high, with May and June as the 2 months with the highest precipitation amounts among all sites (Figure 3). December–January–February, on the other hand, are the months with the least precipitation amount (~47–108 mm/month). January is the driest month on both flanks during the sampled year cycle (Figure 3). The wettest months in the western and eastern flanks are October (211 mm/month) and June (300 mm/month), respectively.

The monthly δ^2H_p and $\delta^{18}O_p$ values from the western flank range from −102.8 to 30.9‰ and −12.7–5.7‰, respectively. On the eastern flank, monthly δ^2H_p and $\delta^{18}O_p$ values range from −108.2 to 7.5‰ and −14.7–4.2‰, respectively (Figure 3). On the western flank, in general, δ^2H_p and $\delta^{18}O_p$ values from December to March are higher than the rest of the year (Figure 3a). We compared annual mean stable isotope values, both with (weighted) and without (unweighted) normalization for precipitation amount, to evaluate the effect of precipitation seasonality on the isotopic signatures in both altitudinal transects (Figures 4a and 4b). Weighted mean δ^2H_p and $\delta^{18}O_p$ values show a stronger correlation (larger R^2) with their corresponding elevation on the western flank than unweighted means (Figures 4a and 4b). For the eastern flank, however, unweighted annual values show a larger R^2 than weighted mean values. The eastern flank shows $R^2 = 0.90$ for δ^2H_p and $R^2 = 0.82$ $\delta^{18}O_p$ when regressed against elevation, but similar regressions for the western flank show little correlation with corresponding R^2 values of 0.07 and 0.05 (Figure 4). For both flanks, precipitation amount correlates better with annual δ^2H_p values, with $R^2 = 0.81$ for the eastern flank and $R^2 = 0.65$ for the western flank, than it does with annual $\delta^{18}O_p$ values (Figure S1 in Supporting Information S1). In addition to the annual values, we compared the weighted seasonal

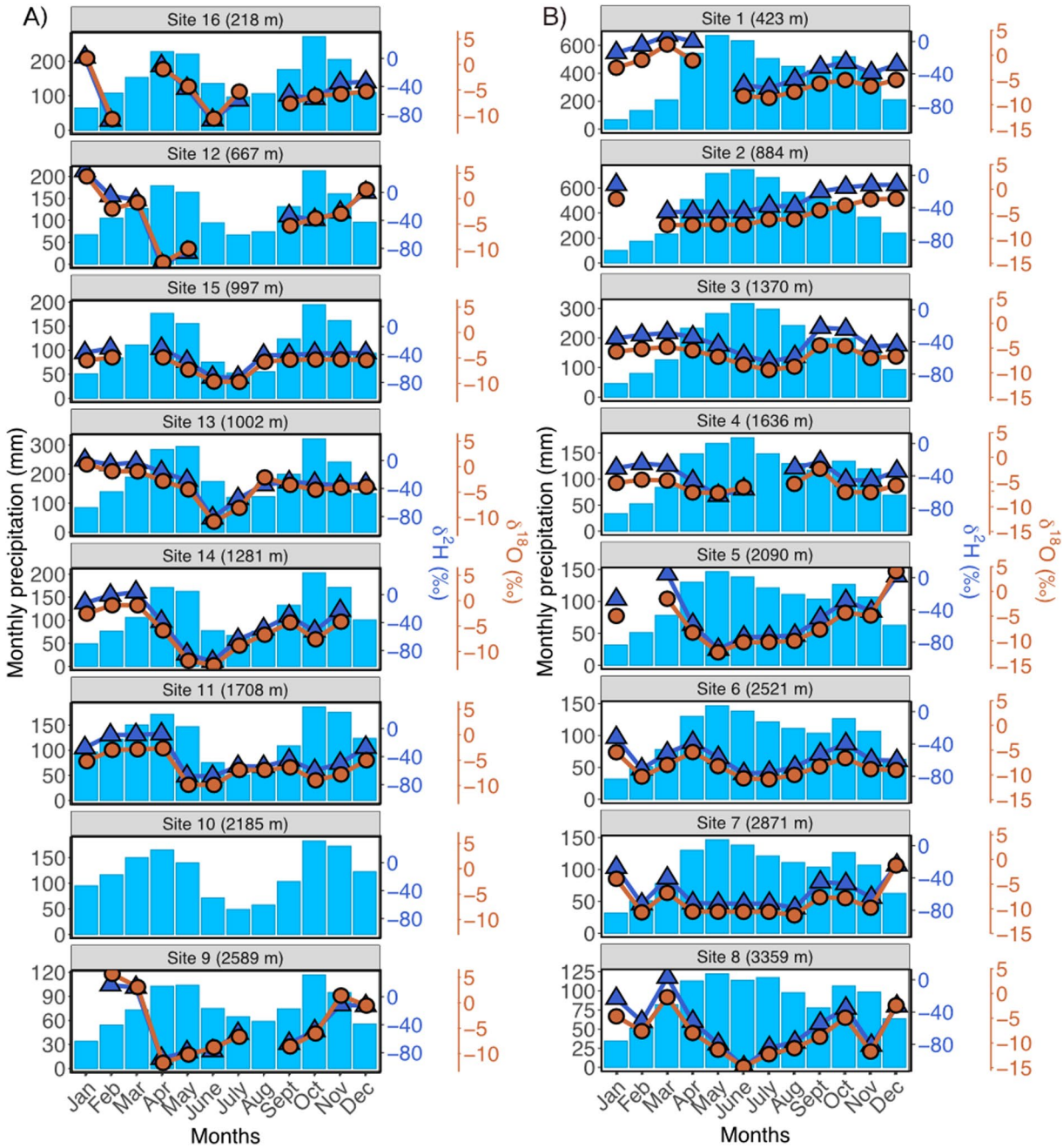

Figure 3. Bar plots of the mean monthly precipitation for the 16 sites along the western (a) and eastern (b) altitudinal transects in the Eastern Cordillera. Blue triangles show the hydrogen isotopes of rainfall and orange circles show the oxygen isotopes of rainfall at these sites. The elevation of each site is shown at the top of its corresponding plot.

δ^2H_p values with elevation for both flanks (Figure S2 in Supporting Information S1). The δ^2H_p values of the wet season in the eastern flank show a higher correlation (R^2 of 0.96) than the weighted annual mean (R^2 of 0.9), but a low correlation with the dry season (R^2 of 0.3) when regressed against elevation. The western flank shows no correlation ($R^2 < 0.05$, p-value >0.2; Figure S2 in Supporting Information S1) when the δ^2H_p values of the wet and dry seasons are regressed against elevation.

The local meteoric water lines (LMWLs) derived from mean monthly values were constructed separately for the wet and dry seasons for each flank (Figures 5a and 5b) (Espinoza et al., 2020; Poveda et al., 2006). In the western flank, the dry season ($\delta^2H_p = 7.0 \times \delta^{18}O_p - 3.6$; $R^2 = 0.93$) and wet season ($\delta^2H_p = 7.1 \times \delta^{18}O_p - 1.5$; $R^2 = 0.91$)

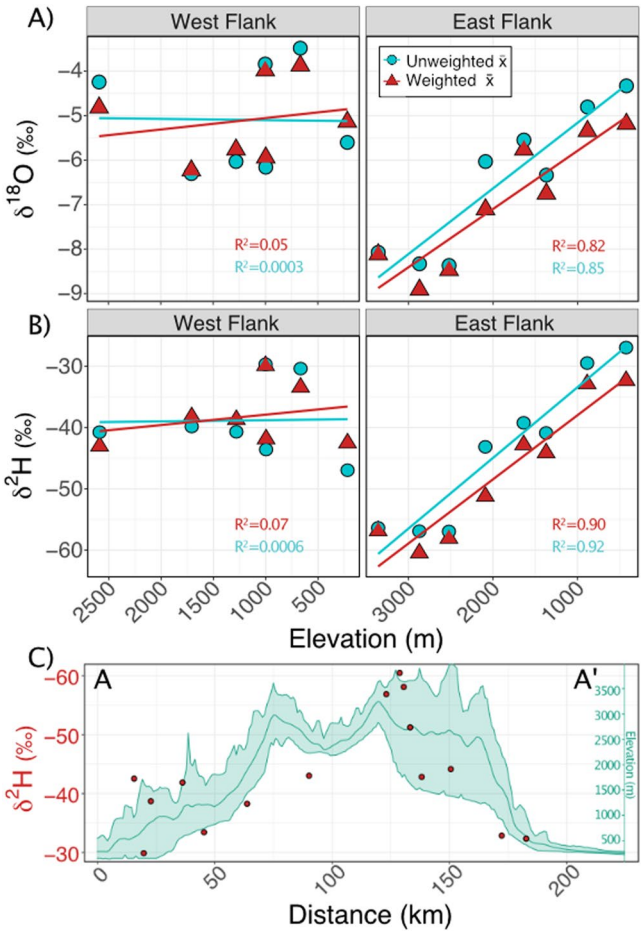

Figure 4. Mean annual stable isotope composition of precipitation in the Eastern Cordillera. (a) Mean annual oxygen isotope values at each site for both flanks vs. elevation. (b) Mean annual hydrogen isotope values of each site for both flanks versus elevation. Light blue dots show the unweighted mean ($\bar{x}$) of monthly values for each site and red triangles show the weighted mean ($\bar{x}$) using the mean annual precipitation amounts from Hurtado-Montoya and Mesa-Sánchez (2014) for each site. (c) Red dots show the mean annual hydrogen isotope values of each site versus distance in the A-A' topographic profile.

LMWLs are similar but have lower slopes and more negative $\delta^{18}O_p$ intercepts than the global meteoric water line (GMWL; solid black line in Figure 5) proposed by Craig (1961) and modified by Rozanski et al. (1993) (δ^2H_p = 8.2(±0.07) × $\delta^{18}O_p$ + 11.27(±0.65)). For the eastern flank, the dry season LMWL ($\delta^2H_p = 5.4 \times \delta^{18}O_p - 7.03$; $R^2 = 0.87$) has a lower slope than the wet season LMWL ($\delta^2H_p = 7.2 \times \delta^{18}O_p + 3.3$; $R^2 = 0.94$), which is closer to the GMWL (Figure 5b). We regressed the annual weighted mean of δ^2H_p against those of $\delta^{18}O_p$ for each station, to assess the difference between the annual LMWLs between the two flanks (Figure 5c) and how they differ from their monthly measurements (Figures 5a and 5b). Overall, the annual LMWL ($\delta^2H_p = 7.4 \times \delta^{18}O_p + 4.5$; $R^2 = 0.95$) of the eastern flank shows a closer fit to the GMWL than the western flank ($\delta^2H_p = 3.3 \times \delta^{18}O_p - 21.4$; $R^2 = 0.4$), which plots to the right of the solid black line (GMWL) in Figure 5c.

To evaluate the efficacy of the stable isotope composition of precipitation as a tool to track overall changes in rainfall amount between years, we plotted the precipitation amount, the δ^2H_p and $\delta^{18}O_p$ annual unweighted and weighted means of each of the 10 years of data (Figure 6a). The year with the highest rainfall amount (year 10 in Figure 6a; 1,234 mm/yr) has the lowest unweighted annual mean δ^2H_p and $\delta^{18}O_p$ values. When plotted as weighted mean δ^2H_p and $\delta^{18}O_p$ values (red line in Figure 6a), however, drier years (e.g., years 3 and 8) exhibit lower values than year 10. Years with the lowest precipitation amount (years 4 and 6 in Figure 6a), on the other hand, do not correspond to the highest δ^2H_p and $\delta^{18}O_p$ values. Additionally, regressions of monthly δ^2H_p and $\delta^{18}O_p$ values of the Bogotá GNIP station with precipitation amounts show R^2 of 0.22 and 0.23, respectively (Figure S3 in Supporting Information S1). The 10-year monthly mean of δ^2H_p and $\delta^{18}O_p$ values of the Bogotá GNIP shows that the month with the lowest values is May (−96‰ and −11.7‰, respectively; Figure 6b). The months with the highest values correspond to January, February, and March with δ^2H_p and $\delta^{18}O_p$ values that range from −28.9‰ to −23.8‰ and −5.4‰ to −4.5‰, respectively (Figure 6b). The two dry seasons in Bogotá have δ^2H_p and $\delta^{18}O_p$ mean values of −31.5‰ and −5.4‰ for December–January–February, and −67.8‰ and −9.7‰ for June–July–August. The two wet seasons, which are March–April–May and September–October–November, have δ^2H_p and $\delta^{18}O_p$ mean values of −64‰ and −8.8‰, and −67.7‰ and −9.9‰, respectively (Figure 6b). Finally, we compared our data against the model of single water vapor source Rayleigh distillation with elevation from Rowley and Garzione (2007) to evaluate how a one-dimensional model captures the isotopic trajectory of precipitation in the Eastern Cordillera of Colombia. We normalized our $\delta^{18}O_p$ annual mean value from each station using the mean value of $\delta^{18}O_p$ from Sao Gabriel GNIP station (0.13°S, 67.08°W, 113m) located in the Amazon basin. Measurements in the eastern flank fall within the 2σ confidence interval of the predicted one-dimensional Rayleigh distillation curve, while more than half of the stations on the western flank do not (Figure 6c).

4.2. δ^2H of Plant Waxes Collected From Soils

We measured the δ^2H_{wax} value of the most abundant, odd numbered, long-chain *n*-alkane homologues (*n*-C_{29}, *n*-C_{31}, and *n*-C_{33}) in top soils along the two elevation transects in the Eastern Cordillera of Colombia. Whereas soils in the eastern flank are dominated by the *n*-C_{31} homologue, we observed no clear dominance on the western flank; each homologue appears to be dominant in at least one site (Figure S4 in Supporting Information S1). To examine the role of this variability on stable isotope compositions, we regressed the δ^2H_{wax} values of each homologue, as well as both the unweighted and weighted (normalized by their concentration, Table S4 in Data Set S1) means at each site against δ^2H_p (Figure 7 and Figure S5 in Supporting Information S1) and elevation (Figure 8). For the eastern flank, only the δ^2H_{wax} values of *n*-C_{29}, and the unweighted mean show a significant

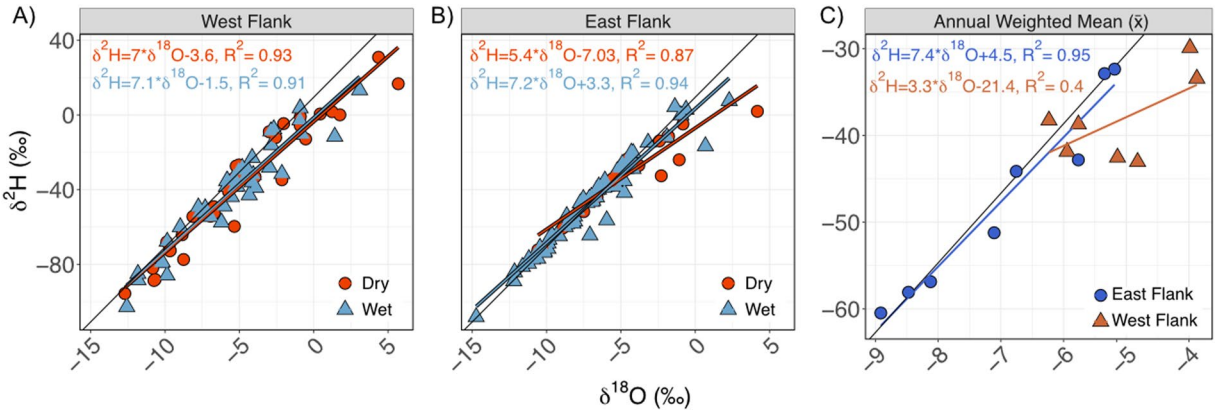

Figure 5. Monthly values of hydrogen versus oxygen stable isotopes in rainfall along the western (a) and eastern (b) altitudinal transects across the Eastern Cordillera. Black lines represent the Global Meteoric Water Line (GMWL). In (a) and (b) each flank is color coded by its corresponding dry and wet seasons; dry months in the west flank correspond to December–January–February and June–July–August, while on the east flank the dry season is defined by December–January–February. (c) Amount-weighted annual means ($\bar{x}$) of δ^2H and $\delta^{18}O$ values for each site. Orange triangles represent the western altitudinal transect and the purple/blue dots the eastern altitudinal transect.

positive correlation with annual δ^2H_p values (p-value = 0.05; Figure 7 and Figure S5 in Supporting Information S1). All δ^2H_{wax} values from the western flank, on the other hand, show no significant correlation with δ^2H_p values ($R^2 < 0.41$, p-value >0.05) (Figure 7 and S5 in Supporting Information S1). To explore the occurrence of a seasonal bias, we regressed the δ^2H_{wax} values of n-C_{29}, n-C_{31}, n-C_{33}, the unweighted mean, and the weighted mean against the weighted seasonal δ^2H_p for each flank (Figure 7 and S5 in Supporting Information S1). In the eastern flank, all δ^2H_{wax} values of n-C_{29}, n-C_{31}, n-C_{33}, the unweighted mean, and weighted mean show a higher correlation with the δ^2H_p of the wet season than with the annual δ^2H_p mean, whereas the western flank shows no significant correlation (p-value >0.05) with any δ^2H_p values (Figure 7 and S5 in Supporting Information S1). Additionally, when excluding the two lowermost sites in the eastern flank, almost all regressions between δ^2H_p and δ^2H_{wax} show higher correlations (larger R^2) than with these two sites included, and have a steeper linear fit (blue diamonds in Figure 7 and Figure S6 in Supporting Information S1).

When regressed against elevation, the δ^2H_{wax} values of n-C_{29}, n-C_{31}, and n-C_{33}, their unweighted means, and their weighted means for the eastern flank decreased by −11.3, −9.0, −7.7, −9.4, and −9.5 ‰ km^{-1}, with R^2 values of 0.64, 0.53, 0.54, 0.65, and 0.63, respectively (Figure 8). For the western flank, however, δ^2H_{wax} values show no significant correlation with elevation ($R^2 < 0.23$, p-value >0.2, Figure 8). Since the unweighted mean δ^2H_{wax} values of n-C_{29}, n-C_{31}, and n-C_{33} in modern soils in the eastern flank exhibited the largest R^2 when regressed against elevation ($R^2 = 0.65$, p-value <0.05, Figure 8), we compared its slope against that of δ^2H_p to calculate a mean $\varepsilon_{wax/p}$ value (Equation 1) for the overall distribution of these n-alkane homologues in soils on that side of the Eastern Cordillera (−137‰, $1\sigma = 4$‰, Figure 9a). Additionally, when comparing the slopes of soil-derived δ^2H_{wax} n-C_{29} elsewhere in the Andes (Figure 9b), the eastern flank of the Eastern Cordillera of Colombia overlaps with the Central Andes of Perú (Feakins et al., 2018; Ponton et al., 2014) with δ^2H_{wax} values ranging from around −155‰ to −210‰, while the South-Central Andes of Argentina show higher δ^2H_{wax} n-C_{29} values of around −110‰ to −160‰ (Nieto-Moreno et al., 2016).

Using Equation (1), we calculated the isotopic fractionation between precipitation and plant waxes ($\varepsilon_{wax/p}$) for n-C_{29}, n-C_{31}, and n-C_{33}, as well as their unweighted and weighted mean for each flank. All $\varepsilon_{wax/p}$ values have a larger dispersion in the western flank compared to the eastern flank (Figure 9c). In general, the $\varepsilon_{wax/p}$ values in the eastern flank are higher ($\varepsilon_{wax/p}$ median of −136‰, $1\sigma = 9$‰) than the western flank ($\varepsilon_{wax/p}$ median of −148‰, $1\sigma = 16$‰; Figure 9c). Also, when regressed with elevation, $\varepsilon_{wax/p}$ values for n-C_{29}, n-C_{31}, and n-C_{33} show more variability in the signal than δ^2H_{wax} values of the same homologues in the eastern flank (Figure S7 in Supporting Information S1). Monthly VPD values range from 0.3 to 1.5 kPa in the eastern flank, and from 0.4 to 1.75 kPa in the western flank (Figure S8 in Supporting Information S1). Additionally, regressions of annual VPD with δ^2H_{wax} values in the eastern flank show a linear correlation ($R^2 > 0.9$) for values lower than 0.8 kPa (Figure S9 in Supporting Information S1). For sites in the western flank, however, annual VPD values show no clear correlation with either of the δ^2H_{wax} values (Figure S9 in Supporting Information S1). When regressing VPD values

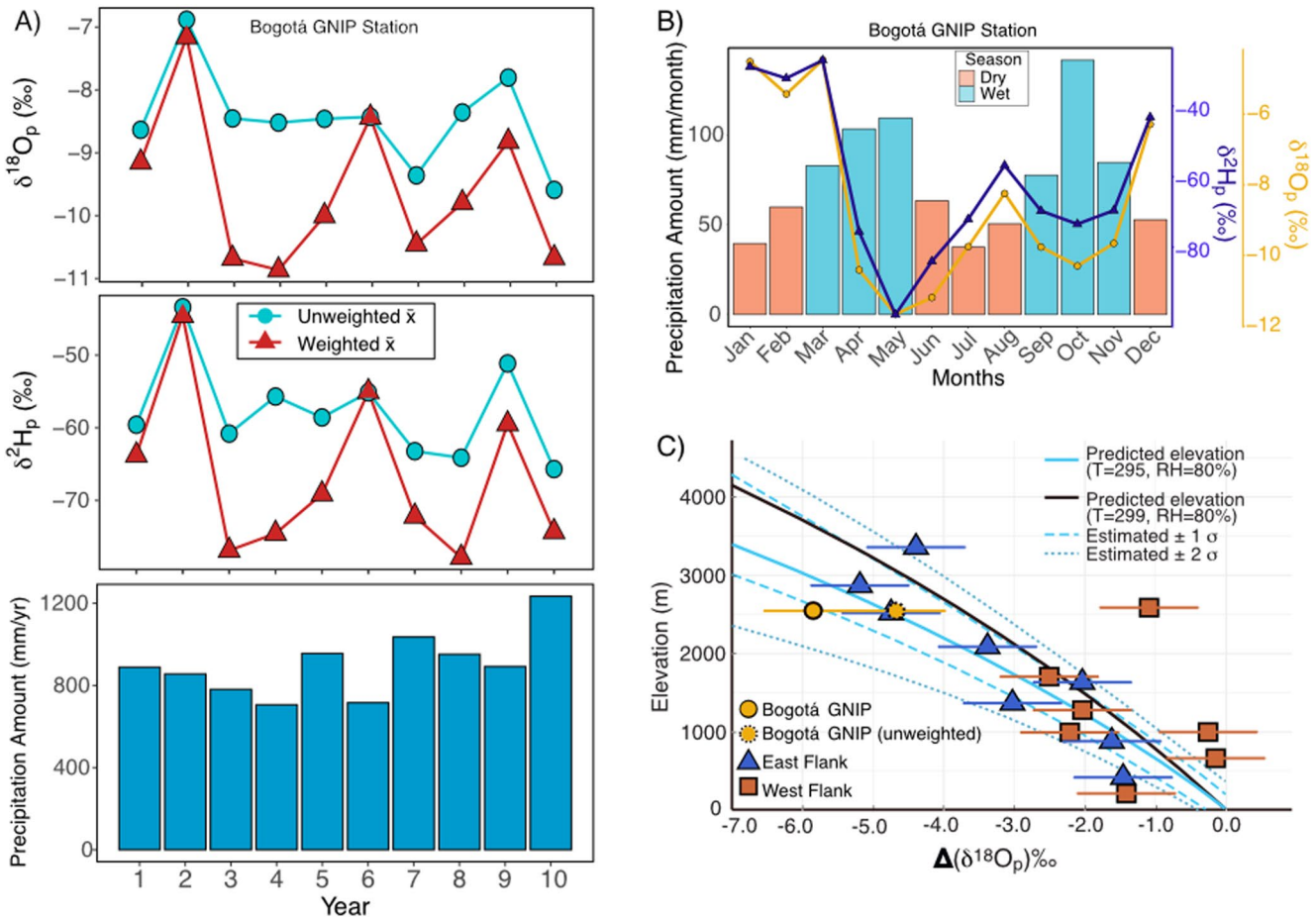

Figure 6. (a) Mean oxygen and hydrogen stable isotope composition of precipitation, and annual precipitation amount of the 10 years with consecutive data from the Bogotá global network of isotopes in precipitation (GNIP) station. Oxygen and hydrogen stable isotope values are both plotted as unweighted mean ($\bar{x}$) (light blue dots) and amount weighted mean ($\bar{x}$) (red triangles). (b) Monthly mean values of oxygen and hydrogen stable isotope composition of precipitation, and precipitation amount from the Bogotá GNIP station. Bar plots of the precipitation amount are color coded by their corresponding seasonality. (c) Rayleigh distillation model for oxygen isotope values versus elevation. All data points are normalized with the average oxygen value from Sao Gabriel GNIP station (89 m.a.s.l) located in the Amazon basin. The error bars correspond to the annual variability of 10 years of data from the Bogotá GNIP station. The light blue line shows predicted values of $\delta^{18}O_p$ for a one-dimensional Rayleigh distillation model with the temperature at sea level of 295K and relative humidity of 80% (RH). Black line is the same one-dimensional model but with an initial temperature of 299K (T). Figure modified from Rowley and Garzione (2007).

of both flanks against δ^2H_{wax} values, a linear correlation persists for VPD values below 0.8 kPa with R^2 of 0.58 (Figure S10 in Supporting Information S1).

5. Discussion

5.1. δ^2H and $\delta^{18}O$ Values of Precipitation and Paleoaltimetry

The stable isotope composition of precipitation along the eastern flank of the Eastern Cordillera of Colombia seems to follow a predicted trajectory of Rayleigh distillation along an ascending trajectory in the region, that is not seen in the western flank (Figure 6c). The correlation of the stable isotope values of precipitation with elevation on the eastern flank (Figure 4) matches the expected trend for Rayleigh distillation during orographic precipitation (Figure 6c), which suggests that this is the main process that controls isotopic fractionation in the eastern flank, consistent with previous work of surface water samples on the same flank (Saylor et al., 2009). Because water vapor sourced from the Atlantic Ocean and the Amazon basin encounters its first topographic barrier on the eastern side of the Eastern Cordillera, variability in stable isotope values of precipitation may result from differences in fractional rainout and temperature change during Rayleigh distillation associated with continentality, elevation, latitude, and precipitation amount. For instance, the linear regression between the δ^2H_p and

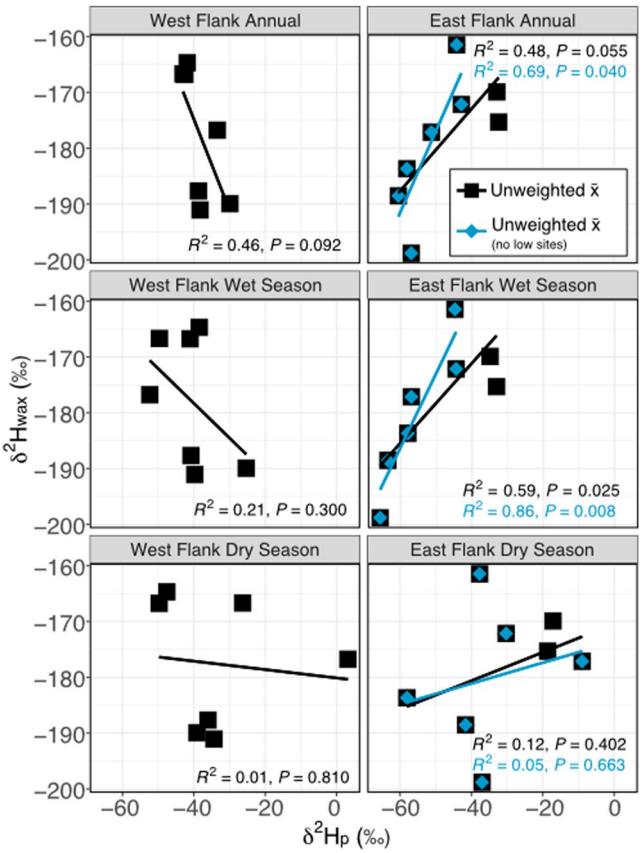

Figure 7. Unweighted δ^2H_{wax} mean ($\bar{x}$) of long-chain *n*-alkane homologues, *n*-C_{29}, *n*-C_{31}, and *n*-C_{33}, in top soils along the two elevation transects in the Eastern Cordillera of Colombia versus δ^2H_p values of mean annual rainfall, the wet season, and the dry season for each site. Blue diamonds show the regressions in the eastern flank excluding the two lower most sites (1 and 2 in Figure 1B). The R^2 and *p*-value of the linear relationship is shown, color-coded for each regression.

$\delta^{18}O_p$ values of the dry season months (December–January–February) on the eastern flank deviates to the right of the GMWL (red line in Figure 5b), suggesting a stronger influence of evaporation on precipitation isotope values compared to the wet season months (Figure 5b). Given that the dry season on the eastern flank includes only 3 months, it is not surprising that the annual mean δ^2H_p and $\delta^{18}O_p$ values follow the GMWL closely (Figure 5c). When regressing the weighted δ^2H_p values of the wet season with elevation, the eastern flank shows a higher correlation ($R^2 = 0.96$) than with the annual weighted mean δ^2H_p values ($R^2 = 0.9$), suggesting that Rayleigh distillation during orographic precipitation has a stronger control on wet season δ^2H_p values than on annual mean δ^2H_p values. The western flank, however, shows no correlation with elevation for either season ($R^2 < 0.05$, Figure S2 in Supporting Information S1).

Because the western slope of the Eastern Cordillera descends into a longitudinal inter-Andean valley, the processes affecting where water vapor condenses and precipitates are more complex than on the eastern flank. The western flank receives moisture from multiple sources that provide water vapor during different seasons throughout the year. Sites in the western flank are not only affected by the remaining Atlantic/Amazon water vapor that passes over the eastern slope of the Eastern Cordillera, but also by water vapor brought from multiple sources. These include the Caribbean low-level jet, the Choco Jet of the Pacific Ocean, particularly during October and November, which are wet season months in the western part of Colombia (Hoyos et al., 2018), in addition to the inter-Andean Magdalena Valley (Figure 1). Thus, the varying water vapor sources throughout the year bring different isotopic signatures, in addition to the already expected variability caused by precipitation amount (Figures 6a and 6b). We corroborated this mixing of sources by analyzing the 10-year monthly mean of the Bogotá GNIP station (Figure 6b). This shows that the difference in δ^2H_p and $\delta^{18}O_p$ values between the two dry seasons, December–January–February and June–July–August, are as big (~30‰) as between any wet season and the December–January–February dry season. In general, δ^2H_p and $\delta^{18}O_p$ values follow the same sinusoidal shape (bimodal seasonality) as the precipitation amount in Bogotá, but there is no difference in the absolute value between the two wet seasons and the June–July–August dry season (Figure 6b). This shows that even if relative changes in stable isotope compositions due to precipitation amount can be seen in the monthly mean, the overprint of water vapor mixing can obscure the interpretation of absolute values of simple Rayleigh distillation over the western flank of the Eastern Cordillera (Figure 6). Additionally, the low correlation ($R^2 \leq 0.23$) between δ^2H_p and $\delta^{18}O_p$ values with precipitation amount in the Bogotá GNIP station (Figure S3 in Supporting Information S1) reflects the influx of multiple water vapor sources.

The lower slope of the LMWL in the western flank of the Eastern Cordillera compared to the slope of the GMWL suggests that precipitation in this region is also affected by evaporation (Figures 5a and 5c). Evaporation and evapotranspiration processes have been shown to play a significant role in the regional water cycle of Colombia, particularly at a seasonal scale in the Magdalena valley (Bedoya-Soto et al., 2019; Durán-Quesada et al., 2012; Poveda & Mesa, 1997). A decrease in evapotranspiration over the Magdalena Valley may be related to a reduction of rainfall from evaporation recycling (Poveda et al., 2006). Bedoya-Soto et al. (2019) showed that evaporation from the bottom of the Magdalena Valley is a source of moisture that contributes to condensation and rainfall during the midnight hours in the June-July-August season. Both our monthly and annual isotope values of precipitation reveal the overprinting of δ^2H_p and $\delta^{18}O_p$ by such evaporation processes in the western flank, as they plot right of the GMWL (Figures 5a and 5c).

The lack of a clear simple Rayleigh distillation process along the western flank (Figure 6c) can also be seen in surface water samples from Saylor et al. (2009). Saylor et al. (2009) excluded Magdalena Valley samples from their meteoric water line equation for the Eastern Cordillera, thus, improving their resulting correlation between

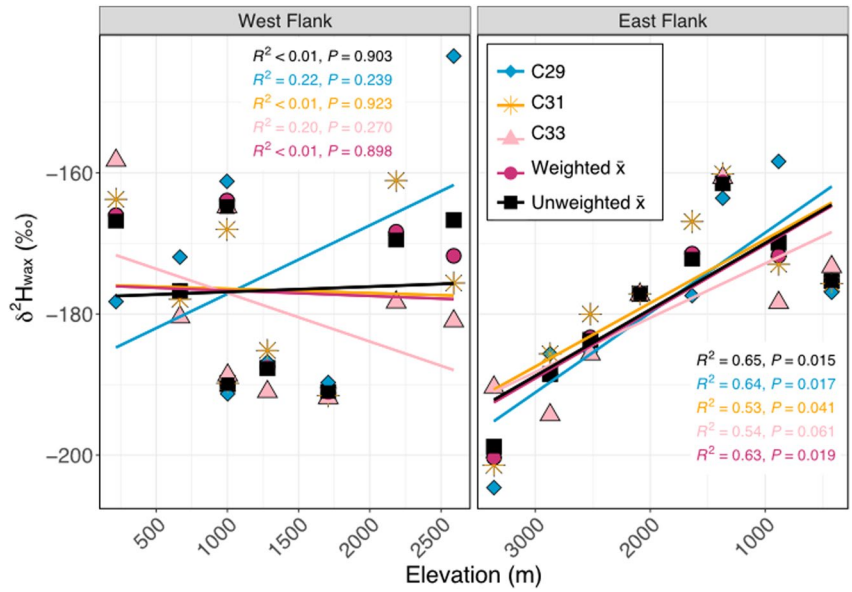

Figure 8. δ^2H_{wax} of long-chain *n*-alkane homologues in top soils along the two elevation transects in the Eastern Cordillera of Colombia. Panels show the δ^2H_{wax} values versus elevation for each site. Blue diamonds represent *n*-C_{29} *n*-alkane, yellow stars *n*-C_{31} *n*-alkanes, pink triangles *n*-C_{33} *n*-alkanes, black squares their unweighted mean ($\bar{x}$), and violet circles their concentration-weighted mean ($\bar{x}$). The R^2 and *p*-value of the linear relationship is shown for each compound.

both $\delta^{18}O$ and δ^2H of surface waters with elevation. This exclusion allowed these authors to conclude that the stable isotope composition of precipitation in the Eastern Cordillera of Colombia can be used for paleoaltimetry studies. When water vapor crosses from the eastern flank (Amazon basin) towards the western flank (Magdalena Valley) over the highest point in the Eastern Cordillera (>3,000 m), the low $\delta^{18}O_p$ and δ^2H_p values at the crest of the eastern flank change to higher values over a short distance west of the crest (Figures 4c and 6). Evidently, the higher $\delta^{18}O_p$ and δ^2H_p values on the western flank require a different source of water from that which condenses farther east. Thus, the isotopic compositions of precipitation and surface water in the western flank of the Eastern Cordillera should be treated with caution for past climate and elevation inferences that rely on such proxies in northern South America.

5.2. δ^2H of *n*-Alkanes and Their Use in Paleoaltimetry

The δ^2H_{wax} values of soil-derived *n*-C_{29}, *n*-C_{31}, and *n*-C_{33} *n*-alkanes from the eastern flank of the Eastern Cordillera decrease systematically with increasing elevation, suggesting that they record the altitude effect seen in precipitation along this transect (Figures 6c and 8). Like other places along the eastern side of the Andes, the δ^2H_{wax} values of *n*-C_{29} on the eastern side of the Eastern Cordillera exhibit the strongest correlation with elevation (R^2 = 0.64, Figure 8). Compared to the Central (~13° S, Feakins et al. [2018]; Ponton et al. [2014]) and South-Central Andes (~25° S, Nieto-Moreno et al. [2016]), where the most abundant *n*-alkane is *n*-C_{29}, the eastern side of the Eastern Cordillera of Colombia is dominated by *n*-C_{31} (Figure S5 in Supporting Information S1). This would suggest potential regional differences in environmental conditions and/or vegetation types that influence the distribution of *n*-alkane homologues in soils. The dependence of δ^2H_{wax} of *n*-C_{29} along the elevation transects varies from −13.2 ‰ km^{-1} in the Central Andes (Perú), −11.3 ‰ km^{-1} in the northern tropical Andes (Colombia, this study), to −9.5 ‰ km^{-1} in the South-Central region (Argentina). The overlap between the northern tropical and Central Andes (Figure 9b) suggests that a similar Rayleigh distillation process, water vapor source initial isotopic composition, and apparent fractionation, over this ~17° latitude range in the eastern slope of the Andes, dominates the δ^2H_{wax} values over any potential differences in environmental conditions and/or plant types. The observed difference between the two northern transects, Colombia (~4°N) and Perú (~13°S), and Argentina (~25°S) (Figure 9b) could be explained by different isotopic compositions of the initial water vapor sources, different apparent fractionation, and/or deep convective processes in the South-Central Andes (Rohrmann et al., 2014). Such differences in the dependence of δ^2H_{wax} values along elevation transects have been

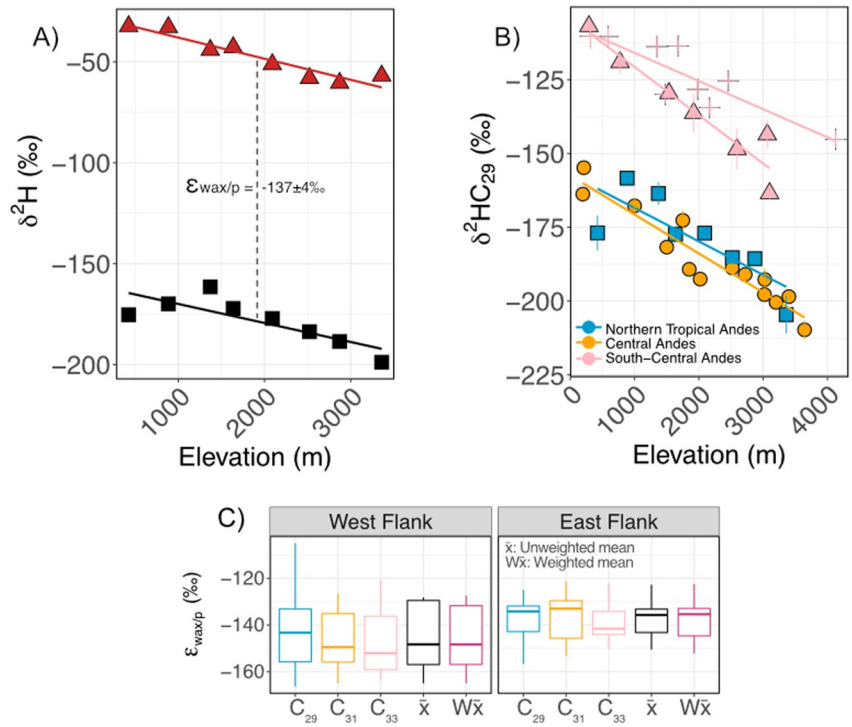

Figure 9. (a) Hydrogen isotopes of rainfall (δ^2H_p, red triangles) and the average of *n*-C_{29}, *n*-C_{31}, and *n*-C_{33} n-alkanes (δ^2H_{wax}, black squares) vs. elevation of the eastern flank of the northern tropical Andes. The average $\varepsilon_{wax/p}$ between the two regressions is −137 ± 4‰. (b) δ^2H_{wax} values of *n*-C_{29} *n*-alkane in soils versus elevation from this study against three other elevation transects along the eastern flank of the Andes. Blue squares represent the eastern flank of the northern tropical Andes (this study), orange dots the Central Andes transect from Feakins et al. (2018), and the pink crosses and triangles the hill and valley transects across the South-Central Andes from Nieto-Moreno et al. (2016). (c) Boxplots showing the median (horizontal line) apparent fractionation ($\varepsilon_{wax/p}$) and the range between the first and third quartile (vertical lines) for *n*-C_{29}, *n*-C_{31}, *n*-C_{33} *n*-alkanes, their unweighted mean ($\bar{x}$), and their concentration-weighted mean ($W\bar{x}$) for each flank.

shown in other mountain regions. Zhang et al. (2017) showed that differences in water vapor sources between a North–South and East–West transect in the Tibetan Plateau are attributed to very distinctive δ^2H_{wax} altitudinal lapse rate (8.7 vs. 22.8 ‰ km^{-1}) values. This is in agreement with previous studies highlighting local environmental conditions and moisture sources as factors to consider when reconstructing past elevations in that region (Bai et al., 2015).

The unweighted mean δ^2H_{wax} values of *n*-C_{29}, *n*-C_{31}, and *n*-C_{33} from the eastern flank exhibit the strongest correlation when regressed against elevation compared to any single homologue (Figure 8). This suggests that the most robust δ^2H_{wax} value to use to calculate paleoelevation estimates in the rock record is the mean of these three homologues. We infer an $\varepsilon_{wax/p}$ (Equation 1) between plant waxes and precipitation in the eastern flank of −137‰ (1σ = 4‰, Figure 9a), which is within the range (−149‰, 1σ = 18‰, to −113‰, 1σ = 31‰) of apparent isotopic fractionation reported for leaf *n*-C_{29} of trees, forbs, and C_3 and C_4 graminoids (Sachse et al., 2012). In future studies, one can use the $\varepsilon_{wax/p}$ in the eastern flank as a proxy to derive estimates of δ^2H_p values from δ^2H_{wax} in the rock record, and thus infer paleo-elevation estimates, assuming similar environmental (i.e., relative humidity) and moisture source (i.e., rainout, moisture recycling, and/or water vapor transport; Winnick et al. [2014]) conditions to today, by using the following equation:

$$\text{Elevation (m)} = -85.9(\pm 11.8) \times \delta^2H_p - 2177.6(\pm 571)\ (R^2 = 0.90,\ p < 0.0005).$$

In contrast, the δ^2H_{wax} values of *n*-alkanes from the western flank of the Eastern Cordillera do not correlate with elevation (Figure 8), which is consistent with the results from δ^2H_p and $\delta^{18}O_p$ values (Figure 4). As previously mentioned, this lack of trend with elevation could be due to the complex atmospheric and topographic configuration of this inter-Andean valley. For paleoaltimetry applications, the δ^2H_{wax} values of long-chain *n*-alkanes in sedimentary archives west of the highest point of the Eastern Cordillera, in our case west of site 8 (~3,400 m,

Figure 1), do not record an elevation-dependent signal. This could explain the lack of evidence for past surface elevation estimates in the Sabana de Bogotá, in the Eastern Cordillera of Colombia, for the past ~7 Ma using δ^2H_{wax} of *n*-C_{29} and *n*-C_{31} reported by Anderson et al. (2015). Since neither $\delta^{18}O_p$ nor δ^2H_p values depend on elevation in the western flank, then the δ^2H_{wax} proxy is unsuitable for paleoaltimetry studies in that region, and possibly in other sediment deposits located in inter-Andean valleys. We thus suggest the use of temperature-dependent proxies such as clumped isotopes in carbonates (Huntington et al., 2015; Snell et al., 2014), branch glycerol dialkyl glycerol tetraethers (brGDGTs; Hren et al. [2010]), or a multi-proxy approach (Garzione et al., 2014) to corroborate and/or replace interpretations in δ^2H_{wax} values.

5.3. δ2H of *n*-Alkanes and Past Hydroclimate Reconstructions

Since global compilations of δ^2H_{wax} values, particularly *n*-C_{29}, exhibit a positive and high correlation (large R^2) with annual δ^2H_p values (Garcin et al., 2012; Hou et al., 2008; McFarlin et al., 2019; Sachse et al., 2006, 2012), the δ^2H_{wax} values from sedimentary records have been used to reconstruct past changes in hydroclimate (Feakins, 2013; Garelick et al., 2021; Konecky et al., 2011; Schefuβ et al., 2005; Tamalavage et al., 2020). In tropical regions, the variability in δ^2H_p and $\delta^{18}O_p$ values are commonly related to the amount of precipitation, with more ^2H-depleted values in areas with higher precipitation amounts (Dansgaard, 1964; Sachse et al., 2012).

As discussed in previous sections, both flanks of the Eastern Cordillera of Colombia show contrasting isotopic signatures. On an annual basis, the regression between the δ^2H_p and δ^2H_{wax} values in the eastern flank has a weak correlation that is marginally significant ($0.05 \leq p$-values ≤ 0.13; Figure 7 and Figure S5 in Supporting Information S1). To evaluate the role of soil evaporation in the incorporation of source water in plants, we regressed the δ^2H_{wax} values with the weighted wet and dry seasonal mean of δ^2H_p. As the δ^2H_{wax} of *n*-C_{29}, *n*-C_{31}, and *n*-C_{33}, as well as their unweighted and weighted means correlate better with the δ^2H_p values of the wet season than the annual or dry δ^2H_p means, we argue that the difference between the δ^2H_p and the δ^2H of soil water is reduced to a minimum during the wet season. This suggests that plants likely incorporate most of their source water during times of reduced evapotranspiration as well as produce more biomass during the wet period. Thus, their δ^2H_{wax} values could be biased towards the wet season. Additionally, we regressed the values of δ^2H_p with δ^2H_{wax} without the two lowermost sites (sites 1 and 2, below 1,500 m.a.s.l. in Figure 1). These sites have the highest mean annual air and soil temperatures, precipitation amount, VPD values, and possibly a plant community distinctive of tropical lowland taxa. When excluding these two sites (blue diamonds in Figure 7), the correlation of the regressions between δ^2H_{wax} and annual and wet season δ^2H_p values show a larger R^2 and p-values <0.05, suggesting that δ^2H_{wax} values in tropical lowland areas could be impacted by higher evapotranspiration rates compared to other elevations. Large differences between δ^2H_p values and δ^2H of soil water are, however, usually seen in places with low precipitation, such as the Chinese Loess Plateau (Liu et al., 2019). In some arid regions, plants have been shown to grow deep roots, which means that they lack the evaporation signal of surface source water (Dawson & Pate, 1996). As sites 1 and 2 in the eastern flank receive twice as much rain as the other sites in our study, we suspect that significant differences in biosynthetic fractionation, possibly related to distinctive plant communities in lowland tropical environments in the northern tropical Andes, could be the main reason for such deviation from linearity in our dataset.

In the western flank, the δ^2H_{wax} of *n*-C_{29}, *n*-C_{31}, and *n*-C_{33}, as well as their unweighted and weighted means, have no significant correlation with δ^2H_p values of either the dry season, wet season, or annual means (p-values >0.05; Figure 7). It is worth noticing that besides their high p-value, the relationship between δ^2H_p and δ^2H_{wax} is negative (Figure 7), which is opposite to the most common direction (positive slope) observed in this correlation elsewhere (Garcin et al., 2012; Polissar & Freeman, 2010; Sachse et al., 2004, 2012). Whereas such negative correlation has been reported in other tropical places like the islands from the South Pacific Convergence Zone (Ladd et al., 2021), an explanation remains elusive. Thus, further studies investigating the modern relationship between δ^2H_p and δ^2H_{wax} in terrestrial tropical regions are needed. For the Eastern Cordillera of Colombia, particularly west of the highest point, δ^2H_{wax} values are not suitable for direct paleo-precipitation estimates, but instead, they reflect a combination of precipitation amount and the stable isotope composition of various moisture sources in this region. Thus, we argue that in sedimentary records from the western flank, and possibly from other inter-Andean valleys, interpretations of past hydroclimate need to be done with caution. We highlight the need for a more robust compilation of modern δ^2H_p and $\delta^{18}O_p$ data of the different water vapor sources in South America for better interpretations of proxy records in the region. Particularly, data from the western margin of

South America would allow us to assess isotopic signatures associated with variations of the ITCZ, the Choco Jet, and possibly other atmospheric circulation features.

Assessing how the composition of plant communities impacts isotopic fractionation and the δ^2H_{wax} values in sedimentary systems is crucial to understand the biological control on isotopic signatures used for paleohydrology and paleoaltimetry. To evaluate the possible role of site-specific factors that could be influencing δ^2H_{wax} values, we regressed the latter with VPD values at each site. As the correlation deviates from linearity with VPD values higher than 0.8 kPa, we infer that the moisture availability above this threshold does not have a systematic impact on δ^2H_{wax} values (see Section 1 in Supporting Information S1). This observation is relevant when interpreting the stable isotope composition of plants (i.e., δ^2H_{wax} or $\delta^{18}O$ of cellulose) to reconstruct VPD changes in areas with values higher than ∼0.8–1.0 kPa. This is because the linear response seen in other studies between these two variables (Kahmen et al., 2011) is lost above this threshold. Thus, we highlight the need for studies on the modern distribution of vegetation in the region to evaluate these relationships. Such studies could provide insights into how changes in plant community (e.g., proportion of monocots vs. dicots) and their associated isotopic fractionation along elevation transects could cause the differences seen in δ^2H_{wax} values in both the western and eastern flanks of the Eastern cordillera of Colombia.

6. Conclusions

We studied the isotopic composition of precipitation (δ^2H_p and $\delta^{18}O_p$) and plant waxes (δ^2H_{wax}) across both flanks of the Eastern Cordillera of the Andes in Colombia to determine their correlation with elevation and their application as a reliable proxy for paleoaltimetry and paleohydrology studies in the region. From our results, we can draw the following conclusions:

1. The stable isotope composition of precipitation in the eastern flank follows a simple Rayleigh distillation process with elevation from a single water vapor source coming from the Atlantic/Amazon basin.
2. The elevation dependencies of δ^2H_p and $\delta^{18}O_p$ are absent along the western flank of the Eastern Cordillera, suggesting that complex atmospheric circulation and water vapor sources, and an inter-Andean location, obscure any simple relationship between precipitation and elevation.
3. The LMWLs slopes, along with the annual weighted mean values of δ^2H_p and $\delta^{18}O_p$, suggest that evaporation processes have a higher impact on the western flank compared to the eastern flank, which contributes to the lack of relationship between δ^2H_p and $\delta^{18}O_p$ and elevation in the western flank.
4. Elevation effects on δ^2H_p in the eastern flank are the main factors in determining the soil-derived δ^2H_{wax} values, which are opposite from the signature seen in the western flank.
5. At a regional level, the δ^2H_{wax} values of n-C_{29} in soil transects from the eastern flank of the Andes show a similar elevation dependency, with the region from Colombia (∼4°N) to Perú (∼13°S) sharing a similar initial water vapor source signature and a simple Rayleigh distillation process. Thus, the δ^2H_{wax} values in the eastern flank of the Andes seem to be suitable for paleoaltimetry studies.
6. We caution against the use of δ^2H_{wax} values for studies that aim to calculate paleoelevation estimates in inter-Andean valleys, like the western flank of the Eastern Cordillera. This is because both δ^2H_p and δ^2H_{wax} values could be impacted by multiple water sources (i.e., more than a single water vapor source, integration of evaporation processes), in addition to biological factors (i.e., plant community composition).
7. In the eastern flank, the δ^2H_{wax} values appear to reflect the isotopic composition of source water from the wet season, giving rise to a possible seasonal bias.
8. In the western flank, δ^2H_p and δ^2H_{wax} values show no significant correlation. The 10-year data of the Bogotá GNIP station, located in the western flank, shows that the different isotopic compositions of moisture sources during different dry seasons could override the overall signature in precipitation amount. Thus, we emphasize caution when interpreting δ^2H_{wax} values to reconstruct past changes in the hydrological cycle in this region.

Data Availability Statement

The Data set S1 is archived in Zenodo data repository and is freely and publicly available online, and may be accessed directly as https://doi.org/10.5281/zenodo.7343372.

Acknowledgments
This research was supported by NSF Sedimentary Geology and Paleobiology Grant 1929199, the Fondo Corrigan ACGGP ARES (Colombia), a Lewis and Clark grant, CIRE's Innovative Research Program (IRP) 2017, a CIRES Graduate Student Research Award, a Figueroa Family Grant from the Graduate School at University of Colorado Boulder, an Edward Fellowship from the Department of Geological Sciences at the University of Colorado Boulder, the DIDI (Dirección de Investigación, Desarrollo e Innovación) from Universidad del Norte, and the Facultad de Ciencias from Universidad de Los Andes (Programa de Investigación C.G). J.S. acknowledges support provided by the University of Colorado Boulder. L.P.A., J.S., and J.J.S. thank the SMART program at University of Colorado Boulder for providing support for a summer internship to J.J.S. We thank Carlos Armando Rosero and Robinson Villamil for assistance in the field, and local residents in Colombia who helped us collect rainfall water samples throughout this research. We thank Sebastian Kopf for access to analytical instrumentation and support on data processing using Isoverse for compound-specific stable isotopic measurements, as well as Bruce Baughn and Valerie Morris for the analysis of water samples. L.P.A. thanks Jamie McFarlin, Sloane Garelick, and Anne Fetrow for valuable discussions about stable isotopes. We thank Prof. Sarah Feakins and an anonymous reviewer for their valuable feedback that improved the manuscript. The data used in this study are listed under Data Availability Statement and cited in the references.

References

Aichner, B., Rajabov, N., Shodmonov, M., Mętrak, M., Suska-Malawska, M., Strecker, M., & Sachse, D. (2021). Local effects on soil leaf wax hydrogen isotopes along a west to east transect through the Pamirs, Tajikistan. *Organic Geochemistry*, *160*, 104272. https://doi.org/10.1016/j.orggeochem.2021.104272

Alvarez-Villa, O. D., Vélez, J. I., & Poveda, G. (2011). Improved long-term mean annual rainfall fields for Colombia. *International Journal of Climatology*, *31*(14), 2194–2212. https://doi.org/10.1002/joc.2232

Anderson, T. A. (1972). Paleogene nonmarine Gualanday Group, Neiva basin, Colombia, and regional development of the Colombian Andes. *The Geological Society of America Bulletin*, *83*(8), 2423–2438. https://doi.org/10.1130/0016-7606(1972)83[2423:pnggnb]2.0.co;2

Anderson, V. J., Saylor, J. E., Shanahan, T. M., & Horton, B. K. (2015). Paleoelevation records from lipid biomarkers: Application to the tropical Andes (pp. 1604–1616). https://doi.org/10.1130/B31105.1.11

Arias, P. A., Garreaud, R., Poveda, G., Espinoza, J. C., Molina-Carpio, J., Masiokas, M., et al. (2021). Hydroclimate of the Andes Part II: Hydroclimate variability and Sub-continental patterns. *Frontiers of Earth Science*, *8*(February), 1–25. https://doi.org/10.3389/feart.2020.505467

Arias, P. A., Martínez, J. A., & Vieira, S. C. (2015). Moisture sources to the 2010-2012 anomalous wet season in northern South America. *Clim. Dyn.*, *45*(9–10), 2861–2884. https://doi.org/10.1007/s00382-015-2511-7

Bai, Y., Fang, X., Gleixner, G., & Mügler, I. (2011). Effect of precipitation regime on δD values of soil n-alkanes from elevation gradients - implications for the study of paleo-elevation. *Organic Geochemistry*, *42*(7), 838–845. https://doi.org/10.1016/j.orggeochem.2011.03.019

Bai, Y., Fang, X., Jia, G., Sun, J., Wen, R., & Ye, Y. (2015). Different altitude effect of leaf wax n-alkane δD values in surface soils along two vapor transport pathways, southeastern Tibetan Plateau. *Geochimica et Cosmochimica Acta*, *170*, 94–107. https://doi.org/10.1016/j.gca.2015.08.016

Bayona, G., Cortés, M., Jaramillo, C., Ojeda, G., Aristizabal, J. J., & Reyes-Harker, A. (2008). An integrated analysis of an orogen-sedimentary basin pair: Latest Cretaceous-Cenozoic evolution of the linked Eastern Cordillera orogen and the Llanos foreland basin of Colombia. *Bulletin of the Geological Society of America*, *120*(9–10), 1171–1197. https://doi.org/10.1130/B26187.1

Bedoya-Soto, J. M., Aristizábal, E., Carmona, A. M., & Poveda, G. (2019). Seasonal shift of the diurnal cycle of rainfall over Mmedellin's valley, central Aandes of Colombia (1998–2005). *Frontiers of Earth Science*, *7*(May). https://doi.org/10.3389/feart.2019.00092

Bendix, J., & Lauer, W. (1992). Die Niederschlagsjahreszeiten in Ecuador undihre klimadynamische interpretation (rainy seasons in Ecuador and their climate- dynamic interpretation). *Erdkunde*, *2*, 118–134.

Blisniuk, P. M., & Stern, L. A. (2005). Stable isotope paleoaltimetry: A critical review. *American Journal of Science*, *305*(10), 1033–1074. https://doi.org/10.2475/ajs.305.10.1033

Chikaraishi, Y., & Naraoka, H. (2003). Compound-specific δD–δ13C analyses of n-alkanes extracted from terrestrial and aquatic plants. *Phytochemistry*, *63*(3), 361–371. https://doi.org/10.1016/s0031-9422(02)00749-5

Craig, H. (1961). Isotopic variations in meteoric waters. *Science*, *133*(3465), 1702–1703. https://doi.org/10.1126/science.133.3465.1702

Dansgaard, W. (1964). Stable isotopes in precipitation. *Tellus*, *16*(4), 436–468. https://doi.org/10.1111/j.2153-3490.1964.tb00181.x

Dawson, T. E., & Pate, J. S. (1996). Seasonal water uptake and movement in root systems of Australian phraeatophytic plants of dimorphic root morphology: A stable isotope investigation. *Oecologia*, *107*(1), 13–20. https://doi.org/10.1007/bf00582230

Diefendorf, A. F., & Freimuth, E. J. (2017). Extracting the most from terrestrial plant-derived n-alkyl lipids and their carbon isotopes from the sedimentary record: A review. *Organic Geochemistry*, *103*, 1–21. https://doi.org/10.1016/j.orggeochem.2016.10.016

Douglas, P. M., Pagani, M., Brenner, M., Hodell, D. A., & Curtis, J. H. (2012). Aridity and vegetation composition are important determinants of leaf-wax δD values in southeastern Mexico and Central America. *Geochimica et Cosmochimica Acta*, *97*, 24–45. https://doi.org/10.1016/j.gca.2012.09.005

Durán-Quesada, A. M., Reboita, M., & Gimeno, L. (2012). Brève revue des précipitations en amérique tropicale et des sources d'humidité associées. *Hydrological Sciences Journal*, *57*(4), 612–624. https://doi.org/10.1080/02626667.2012.673723

Eglinton, G., & Hamilton, R. J. (1967). Leaf epicuticular waxes. *Science*, *156*(3780), 1322–1335. https://doi.org/10.1126/science.156.3780.1322

Eglinton, T. I., & Eglinton, G. (2008). Molecular proxies for paleoclimatology. *Earth and Planetary Science Letters*, *275*(1–2), 1–16. https://doi.org/10.1016/j.epsl.2008.07.012

Espinoza, J. C., Garreaud, R., Poveda, G., Arias, P. A., Molina-Carpio, J., Masiokas, M., et al. (2020). Hydroclimate of the Andes Part I: Main climatic features. *Frontiers of Earth Science*, *8*(March), 1–20. https://doi.org/10.3389/feart.2020.00064

Espinoza, J. C., Ronchail, J., Guyot, J. L., Cochonneau, G., Naziano, F., Lavado, W., et al. (2009). Spatio-temporal rainfall variability in the Amazon basin countries (Brazil, Peru, Bolivia, Colombia, and Ecuador). *International Journal of Climatology*, *29*(11), 1574–1594. https://doi.org/10.1002/joc.1791

Feakins, S. J. (2013). Pollen-corrected leaf wax D/H reconstructions of northeast African hydrological changes during the late Miocene. *Palaeogeography, Palaeoclimatology, Palaeoecology*, *374*, 62–71. https://doi.org/10.1016/j.palaeo.2013.01.004

Feakins, S. J., Martin, R. E., Shenkin, A., Asner, G. P., Peters, T., Wu, M. S., et al. (2016). Plant leaf wax biomarkers capture gradients in hydrogen isotopes of precipitation from the Andes and Amazon. *Geochimica et Cosmochimica Acta*, *182*, 155–172. https://doi.org/10.1016/j.gca.2016.03.018

Feakins, S. J., & Sessions, A. L. (2010). Controls on the D/H ratios of plant leaf waxes in an arid ecosystem. *Geochimica et Cosmochimica Acta*, *74*(7), 2128–2141. https://doi.org/10.1016/j.gca.2010.01.016

Feakins, S. J., Wu, M. S., Ponton, C., Galy, V., & West, A. J. (2018). Dual isotope evidence for sedimentary integration of plant wax biomarkers across an Andes-Amazon elevation transect. *Geochimica et Cosmochimica Acta*, *242*, 64–81. https://doi.org/10.1016/j.gca.2018.09.007

Freimuth, E. J., Diefendorf, A. F., & Lowell, T. V. (2017). Hydrogen isotopes of n-alkanes and n-alkanoic acids as tracers of precipitation in a temperate forest and implications for paleorecords. *Geochimica et Cosmochimica Acta*, *206*, 166–183. https://doi.org/10.1016/j.gca.2017.02.027

Garcin, Y., Schwab, V. F., Gleixner, G., Kahmen, A., Todou, G., Séné, O., et al. (2012). Hydrogen isotope ratios of lacustrine sedimentary n-alkanes as proxies of tropical African hydrology: Insights from a calibration transect across Cameroon. *Geochimica et Cosmochimica Acta*, *79*, 106–126. https://doi.org/10.1016/j.gca.2011.11.039

Garelick, S., Russell, J. M., Dee, S., Verschuren, D., & Olago, D. O. (2021). Atmospheric controls on precipitation isotopes and hydroclimate in high-elevation regions in Eastern Africa since the Last Glacial Maximum. *Earth and Planetary Science Letters*, *567*, 116984. https://doi.org/10.1016/j.epsl.2021.116984

Garzione, C. N., Auerbach, D. J., Smith, J. J. S., Rosario, J. J., Passey, B. H., Jordan, T. E., & Eiler, J. M. (2014). Clumped isotope evidence for diachronous surface cooling of the Altiplano and pulsed surface uplift of the Central Andes. *Earth and Planetary Science Letters*, *393*, 173–181. https://doi.org/10.1016/j.epsl.2014.02.029

Garzione, C. N., Dettman, D. L., Quade, J., De Celles, P. G., & Butler, R. F. (2000). High times on the Tibetan plateau: Paleoelevation of the Thakkhola graben, Nepal. *Geology*, *28*(4), 339–342. https://doi.org/10.1130/0091-7613(2000)28<339:HTOTTP>2.0.CO;2

Garzione, C. N., Quade, J., DeCelles, P. G., & English, N. B. (2000). Predicting paleoelevation of Tibet and the Himalaya from δ18O vs. altitude gradients in meteoric water across the Nepal Himalaya. *Earth and Planetary Science Letters*, *183*(1–2), 215–229. https://doi.org/10.1016/S0012-821X(00)00252-1

Goldsmith, Y., Polissar, P. J., de Menocal, P. B., & Broecker, W. S. (2019). Leaf wax δD and δ13C in soils record hydrological and environmental Information across a climatic gradient in Israel. *Journal of Geophysical Research: Biogeosciences*, *124*(9), 2898–2916. https://doi.org/10.1029/2019JG005149

Helmens, K. F., & van der Hammen, T. (1994). The pliocene and quaternary of the high plain of Bogotá (Colombia): A history of tectonic uplift, basin development and climatic change. *Quaternary International*, *21*(C), 41–61. https://doi.org/10.1016/1040-6182(94)90020-5

Hooghiemstra, H., Wijninga, V. M., & Cleef, A. M. (2006). The paleobotanical record of Colombia: Implications for biogeography and biodiversity 1. *Annals of the Missouri Botanical Garden*, *93*(2), 297–325. https://doi.org/10.3417/0026-6493(2006)93[297:tproci]2.0.co;2

Hou, J., D'Andrea, W. J., & Huang, Y. (2008). Can sedimentary leaf waxes record D/H ratios of continental precipitation? Field, model, and experimental assessments. *Geochimica et Cosmochimica Acta*, *72*(14), 3503–3517. https://doi.org/10.1016/j.gca.2008.04.030

Hoyos, I., Dominguez, F., Cañón-Barriga, J., Martínez, J. A., Nieto, R., Gimeno, L., & Dirmeyer, P. A. (2018). Moisture origin and transport processes in Colombia, northern South America. *Climate Dynamics*, *50*(3–4), 971–990. https://doi.org/10.1007/s00382-017-3653-6

Hren, M. T., Pagani, M., Erwin, D. M., & Brandon, M. (2010). Biomarker reconstruction of the early Eocene paleotopography and paleoclimate of the northern Sierra Nevada. *Geology*, *38*(1), 7–10. https://doi.org/10.1130/G30215.1

Huntington, K. W., Saylor, J., Quade, J., & Hudson, A. M. (2015). High late Miocene–Pliocene elevation of the Zhada Basin, southwestern Tibetan Plateau, from carbonate clumped isotope thermometry. *Bulletin*, *127*(1–2), 181–199. https://doi.org/10.1130/b31000.1

Hurtado-Montoya, A. F., & Mesa-Sánchez, Ó. J. (2014). Reanalysis of monthly precipitation fields in Colombian territory. *Dyna*, *81*(186), 251. https://doi.org/10.15446/dyna.v81n186.40419

Jackson, L. J., Horton, B. K., Beate, B. O., Bright, J., & Breecker, D. O. (2019). Testing stable isotope paleoaltimetry with Quaternary volcanic glasses from the Ecuadorian Andes. *Geology*, *47*(March), 1–414. –5. https://doi.org/10.1130/G45861.1

Jaeschke, A., Rethemeyer, J., Lappé, M., Schouten, S., Boeckx, P., & Schefuß, E. (2018). Influence of land use on distribution of soil n-alkane δD and brGDGTs along an altitudinal transect in Ethiopia: Implications for (paleo)environmental studies. *Organic Geochemistry*, *124*, 77–87. https://doi.org/10.1016/j.orggeochem.2018.06.006

Kahmen, A., Sachse, D., Arndt, S. K., Tu, K. P., Farrington, H., Vitousek, P. M., & Dawson, T. E. (2011). Cellulose δ18O is an index of leaf-to-air vapor pressure difference (VPD) in tropical plants. *Proceedings of the National Academy of Sciences*, *108*(5), 1981–1986. https://doi.org/10.1073/pnas.1018906108

Kar, N., Garzione, C. N., Jaramillo, C., Shanahan, T., Carlotto, V., Pullen, A., et al. (2016). Rapid regional surface uplift of the northern Altiplano plateau revealed by multiproxy paleoclimate reconstruction. *Earth and Planetary Science Letters*, *447*, 33–47. https://doi.org/10.1016/j.epsl.2016.04.025

Konecky, B. L., Russell, J. M., Johnson, T. C., Brown, E. T., Berke, M. A., Werne, J. P., & Huang, Y. (2011). Atmospheric circulation patterns during late Pleistocene climate changes at Lake Malawi, Africa. *Earth and Planetary Science Letters*, *312*(3–4), 318–326. https://doi.org/10.1016/j.epsl.2011.10.020

Kopf, S., Davidheiser-Kroll, B., & Kocken, I. (2021). Isoreader: An R package to read stable isotope data files for reproducible research. *Journal of Open Source Software*, *6*(61), 2878. https://doi.org/10.21105/joss.02878

Krull, E., Sachse, D., Mügler, I., Thiele, A., & Gleixner, G. (2006). Compound-specific δ13C and δ2H analyses of plant and soil organic matter: A preliminary assessment of the effects of vegetation change on ecosystem hydrology. *Soil Biology and Biochemistry*, *38*(11), 3211–3221. https://doi.org/10.1016/j.soilbio.2006.04.008

Ladd, S. N., Maloney, A. E., Nelson, D. B., Prebble, M., Camperio, G., Sear, D. A., et al. (2021). Leaf wax hydrogen isotopes as a hydroclimate proxy in the tropical Pacific. *Journal of Geophysical Research: Biogeosciences*, *126*(3), 1–21. https://doi.org/10.1029/2020JG005891

Li, L., & Garzione, C. N. (2017). Spatial distribution and controlling factors of stable isotopes in meteoric waters on the Tibetan Plateau: Implications for paleoelevation reconstruction. *Earth and Planetary Science Letters*, *460*, 302–314. https://doi.org/10.1016/j.epsl.2016.11.046

Liu, W., Wang, H., Leng, Q., Liu, H., Zhang, H., Xing, M., et al. (2019). Hydrogen isotopic compositions along a precipitation gradient of Chinese Loess Plateau: Critical roles of precipitation/evaporation and vegetation change as controls for leaf wax δD. *Chemical Geology*, *528*, 119278. https://doi.org/10.1016/j.chemgeo.2019.119278

Luo, P., Peng, P., Gleixner, G., Zheng, Z., Pang, Z., & Ding, Z. (2011). Empirical relationship between leaf wax n-alkane δD and altitude in the Wuyi, Shennongjia and Tianshan Mountains, China: Implications for paleoaltimetry. *Earth and Planetary Science Letters*, *301*(1–2), 285–296. https://doi.org/10.1016/j.epsl.2010.11.012

McFarlin, J. M., Axford, Y., Masterson, A. L., & Osburn, M. R. (2019). Calibration of modern sedimentary δ2H plant wax-water relationships in Greenland lakes. *Quaternary Science Reviews*, *225*, 105978. https://doi.org/10.1016/j.quascirev.2019.105978

Mejia, J. F., Mesa, O., Poveda, G., & Velez, J. I. (1999). Distribución espacial y ciclos anual y semianual de la precipitación en Colombia. *Dyna*, *127*, 7–14.

Molnar, P., & Pérez-Angel, L. C. (2021). Constraints on the paleoelevation history of the Eastern Cordillera of Colombia from its palynological record. *Geosphere*, *17*(4), 1333–1352. https://doi.org/10.1130/ges02328.1

Mora, A., Parra, M., Strecker, M. R., Sobel, E. R., Hooghiemstra, H., Torres, V., & Jaramillo, J. V. (2008). Climatic forcing of asymmetric orogenic evolution in the Eastern Cordillera of Colombia. *Bulletin of the Geological Society of America*, *120*(7–8), 930–949. https://doi.org/10.1130/B26186.1

Mora-Páez, H., Mencin, D. J., Molnar, P., Diederix, H., Cardona-Piedrahita, L., Peláez-Gaviria, J.-R., & Corchuelo-Cuervo, Y. (2016). GPS velocities and the construction of the eastern cordillera of the Colombian Andes. *Geophysical Research Letters*, *43*(16), 8407–8416. https://doi.org/10.1002/2016GL069795

Mulch, A., Sarna-Wojcicki, A. M., Perkins, M. E., & Chamberlain, C. P. (2008). A Miocene to Pleistocene climate and elevation record of the Sierra Nevada (California). *Proceedings of the National Academy of Sciences of the United States of America*, *105*(19), 6819–6824. https://doi.org/10.1073/pnas.0708811105

Nieto-Moreno, V., Rohrmann, A., van der Meer, M. T. J., Sinninghe Damsté, J. S., Sachse, D., Tofelde, S., et al. (2016). Elevation-dependent changes in n-alkane δD and soil GDGTs across the South Central Andes. *Earth and Planetary Science Letters*, *453*, 234–242. https://doi.org/10.1016/j.epsl.2016.07.049

Pagani, M., Pedentchouk, N., Huber, M., Sluijs, A., Schouten, S., Brinkhuis, H., et al. (2006). Arctic hydrology during global warming at the Palaeocene/Eocene thermal maximum. *Nature*, *442*(7103), 671–675. https://doi.org/10.1038/nature05043

Pérez-Angel, L. C., & Molnar, P. (2017). Sea surface temperature in the Eastern equatorial Pacific and surface temperature in the Eastern Cordillera of Colombia during El Nino: Implications of Pliocene conditions. *Paleoceanography and Paleoclimatology*, *32*(11), 1309–1314. https://doi.org/10.1002/2017PA003182

Pérez-Angel, L., Sepúlveda, J., Molnar, P., Montes, C., Rajagopalan, B., Snell, K., et al. (2020). Soil and air temperature calibrations using branched GDGTs for the Tropical Andes of Colombia: Towards a pan-tropical calibration. *Geochemistry, Geophysics, Geosystems*, *21*(8), 1–18. https://doi.org/10.1029/2020GC008941

Polissar, P. J., & Freeman, K. H. (2010). Effects of aridity and vegetation on plant-wax δD in modern lake sediments. *Geochimica et Cosmochimica Acta*, *74*(20), 5785–5797. https://doi.org/10.1016/j.gca.2010.06.018

Polissar, P. J., Freeman, K. H., Rowley, D. B., McInerney, F. A., & Currie, B. S. (2009). Paleoaltimetry of the Tibetan Plateau from D/H ratios of lipid biomarkers. *Earth and Planetary Science Letters*, *287*(1–2), 64–76. https://doi.org/10.1016/j.epsl.2009.07.037

Ponton, C., West, A. J., Feakins, S. J., & Galy, V. (2014). Leaf wax biomarkers in transit record river catchment composition. *Geophysical Research Letters*, *41*(18), 6420–6427. https://doi.org/10.1002/2014GL061328

Poveda, G., Jaramillo, A., Gil, M. M., Quiceno, N., & Mantilla, R. I. (2001). Seasonality in ENSO-related precipitation, river discharges, soil moisture, and vegetation index in Colombia. *Water Resources Research*, *37*(8), 2169–2178. https://doi.org/10.1029/2000WR900395

Poveda, G., & Mesa, O. (2000). On the existence of Lloró (the rainiest locality on Earth): Enhanced ocean-land-atmosphere interaction by a low-level jet. *Geophysical Research Letters*, *27*(11), 1675–1678. https://doi.org/10.1029/1999gl006091

Poveda, G., & Mesa, O. J. (1997). Feedbacks between hydrological processes in tropical South America and large-scale ocean-atmospheric phenomena. *Journal of Climate*, *10*(10), 2690–2702. https://doi.org/10.1175/1520-0442(1997)010<2690:FBHPIT>2.0.CO;2

Poveda, G., Waylen, P. R., & Pulwarty, R. S. (2006). Annual and inter-annual variability of the present climate in northern South America and southern Mesoamerica. *Palaeogeography, Palaeoclimatology, Palaeoecology*, *234*(1), 3–27. https://doi.org/10.1016/j.palaeo.2005.10.031

Ricaurte, L. F., Patiño, J. E., Zambrano, D. F. R., Arias-G, J. C., Acevedo, O., Aponte, C., et al. (2019). A classification system for Colombian eetlands: An essential step forward in open environmental policy-making. *Wetlands*, *39*(5), 971–990. https://doi.org/10.1007/s13157-019-01149-8

Rodríguez, C. (2004). Línea Meteórica Isotópica de Colombia. *Meteorología Colombiana*(8), 43–51.

Rohrmann, A., Strecker, M. R., Bookhagen, B., Mulch, A., Sachse, D., Pingel, H., et al. (2014). Can stable isotopes ride out the storms? The role of convection for water isotopes in models, records, and paleoaltimetry studies in the central Andes. *Earth and Planetary Science Letters*, *407*, 187–195. https://doi.org/10.1016/j.epsl.2014.09.021

Rowley, D. B. (2007). Stable isotope-based paleoaltimetry: Theory and validation. *Reviews in Mineralogy and Geochemistry*, *66*(1), 23–52. https://doi.org/10.2138/rmg.2007.66.2

Rowley, D. B. (2018). Stable isotope-based paleoaltimetry: Theory and validation. *Paleoaltimetry: Geochemical and Thermodynamic Approaches*, *66*(1), (1998), 23–52. https://doi.org/10.2138/rmg.2007.66.2

Rowley, D. B., & Garzione, C. N. (2007). Stable isotope-based paleoaltimetry. *Annual Review of Earth and Planetary Sciences*, *35*(1), 463–508. https://doi.org/10.1146/annurev.earth.35.031306.140155

Rowley, D. B., Pierrehumbert, R. T., & Currie, B. S. (2001). A new approach to stable isotope-based paleoaltimetry: Implications for paleoaltimetry and paleohypsometry of the High Himalaya since the late Miocene. *Earth and Planetary Science Letters*, *188*(1–2), 253–268. https://doi.org/10.1016/S0012-821X(01)00324-7

Rozanski, K., Araguás-Araguás, L., & Gonfiantini, R. (1993). Isotopic patterns in modern global precipitation. *Geophysical Monograph-American Geophysical Union*, *78*, 1-1.

Sachse, D., Billault, I., Bowen, G. J., Chikaraishi, Y., Dawson, T. E., Feakins, S. J., et al. (2012). Molecular paleohydrology: Interpreting the hydrogen-isotopic composition of lipid biomarkers from photosynthesizing organisms. *Annual Review of Earth and Planetary Sciences*, *40*(1), 221–249. https://doi.org/10.1146/annurev-earth-042711-105535

Sachse, D., Radke, J., & Gleixner, G. (2004). Hydrogen isotope ratios of recent lacustrine sedimentary n-alkanes record modern climate variability. *Geochimica et Cosmochimica Acta*, *68*(23), 4877–4889. https://doi.org/10.1016/j.gca.2004.06.004

Sachse, D., Radke, J., & Gleixner, G. (2006). δD values of individual n-alkanes from terrestrial plants along a climatic gradient–Implications for the sedimentary biomarker record. *Organic Geochemistry*, *37*(4), 469–483. https://doi.org/10.1016/j.orggeochem.2005.12.003

Sauer, P. E., Eglinton, T. I., Hayes, J. M., Schimmelmann, A., & Sessions, A. L. (2001). Compound-specific D/H ratios of lipid biomarkers from sediments as a proxy for environmental and climatic conditions. *Geochimica et Cosmochimica Acta*, *65*(2), 213–222. https://doi.org/10.1016/s0016-7037(00)00520-2

Saylor, J. E., Mora, A., Horton, B. K., & Nie, J. (2009). Controls on the isotopic composition of surface water and precipitation in the Northern Andes, Colombian Eastern Cordillera. *Geochimica et Cosmochimica Acta*, *73*(23), 6999–7018. https://doi.org/10.1016/j.gca.2009.08.030

Schefuß, E., Schouten, S., & Schneider, R. R. (2005). Climatic controls on central African hydrology during the past 20, 000 years. *Nature*, *437*(7061), 1003–1006. https://doi.org/10.1038/nature03945

Sierra, J. P., Arias, P. A., Durán-Quesada, A. M., Tapias, K. A., Vieira, S. C., & Martínez, J. A. (2021). The Choco low-level jet: Past, present and future. *Climate Dynamics*, *56*(7–8), 2667–2692. https://doi.org/10.1007/s00382-020-05611-w

Sierra, J. P., Arias, P. A., & Vieira, S. C. (2015). Precipitation over northern South America and its seasonal variability as simulated by the CMIP5 models. *Advances in Meteorology*, *2015*, 1–22. https://doi.org/10.1155/2015/634720

Smith, F. A., & Freeman, K. H. (2006). Influence of physiology and climate on δD of leaf wax n-alkanes from C3 and C4 grasses. *Geochimica et Cosmochimica Acta*, *70*(5), 1172–1187. https://doi.org/10.1016/j.gca.2005.11.006

Snell, K. E., Koch, P. L., Druschke, P., Foreman, B. Z., & Eiler, J. M. (2014). High elevation of the 'Nevadaplano' during the late Cretaceous. *Earth and Planetary Science Letters*, *386*, 52–63. https://doi.org/10.1016/j.epsl.2013.10.046

Super, J. R., Chin, K., Pagani, M., Li, H., Tabor, C., Harwood, D. M., et al. (2018). Late Cretaceous climate in the Canadian Arctic: Multi-proxy constraints from Devon island. *Palaeogeography, Palaeoclimatology, Palaeoecology*, *504*, 1–22. https://doi.org/10.1016/j.palaeo.2018.03.004

Tamalavage, A. E., van Hengstum, P. J., Louchouarn, P., Fall, P. L., Donnelly, J. P., Albury, N. A., et al. (2020). Plant wax evidence for precipitation and vegetation change from a coastal sinkhole lake in the Bahamas spanning the last 3000 years. *Organic Geochemistry*, *150*, 104120. https://doi.org/10.1016/j.orggeochem.2020.104120

Tierney, J. E., Russell, J. M., Huang, Y., Sinninghe Damsté, J. S., Hopmans, E. C., & Cohen, A. S. (2008). Northern hemisphere controls on tropical southeast African climate during the past 60, 000 years. *Science*, *322*(5899), 252–255. https://doi.org/10.1126/science.1160485

Urrea, V., Ochoa, A., & Mesa, O. (2019). Seasonality of rainfall in Colombia. *Water Resources Research*, *55*(5), 4149–4162. https://doi.org/10.1029/2018WR023316

Van der Hammen, T., Werner, J. H., & van Dommelen, H. (1973). Palynological record of the upheaval of the northern Andes: A study of the pliocene and lower quaternary of the Colombian eastern cordillera and the early evolution of its high-Andean biota. *Review of Palaeobotany and Palynology*, *16*(1–2), 1–42. https://doi.org/10.1016/0034-6667(73)90031-6

Wang, C., Hren, M. T., Hoke, G. D., Liu-Zeng, J., & Garzione, C. N. (2017). Soil n-alkane δD and glycerol dialkyl glycerol tetraether (GDGT) distributions along an altitudinal transect from southwest China: Evaluating organic molecular proxies for paleoclimate and paleoelevation. *Organic Geochemistry*, *107*, 21–32. https://doi.org/10.1016/j.orggeochem.2017.01.006

Wijninga, V. M. (1996). Neogene ecology of the Salto de Tequendama site (2475 m altitude, Cordillera Oriental, Colombia): The paleobotanical record of montane and lowland forests. *Review of Palaeobotany and Palynology*, *92*(1–2), 97–156. https://doi.org/10.1016/0034-6667(94)00100-6

Wijninga, V. M., & Kuhry, P. (1990). A pliocene flora from the Subachoque valley (cordillera Oriental, Colombia). *Review of Paleobotany and Palynology*, *62*(3–4), 249–290.

Williford, K. H., Grice, K., Alexander, H., & McElwain, J. C. (2014). An organic record of terrestrial ecosystem collapse and recovery at the Triassic–Jurassic boundary in East Greenland. *Geochimica et Cosmochimica Acta*, *127*, 251–263. https://doi.org/10.1016/j.gca.2013.11.033

Winnick, M. J., Chamberlain, C. P., Caves, J. K., & Welker, J. M. (2014). Quantifying the isotopic 'continental effect. *Earth and Planetary Science Letters*, *406*, 123–133. https://doi.org/10.1016/j.epsl.2014.09.005

Zhang, X., Xu, B., Günther, F., Mügler, I., Lange, M., Zhao, H., et al. (2017). Hydrogen isotope ratios of terrestrial leaf wax n-alkanes from the Tibetan Plateau: Controls on apparent enrichment factors, effect of vapor sources and implication for altimetry. *Geochimica et Cosmochimica Acta*, *211*, 10–27. https://doi.org/10.1016/j.gca.2017.04.035

References From the Supporting Information

Brun, P., Zimmermann, N. E., Hari, C., Pellissier, L., & Karger, D. N. (2022). Global climate-related predictors at kilometre resolution for the past and future. *Earth System Science Data Discussions*, 1–44.

Eley, Y. L., & Hren, M. T. (2018). Reconstructing vapor pressure deficit from leaf wax lipid molecular distributions. *Scientific Reports*, *8*(1), 1–8. https://doi.org/10.1038/s41598-018-21959-w

Hooghiemstra, H., & Van Der Hammen, T. (1998). Neogene and Quaternary development of the neotropical rain forest: The forest refugia hypothesis, and a literature overview. *Earth-Science Reviews*, *44*(3–4), 147–183. https://doi.org/10.1016/S0012-8252(98)00027-0

Sachse, D., Gleixner, G., Wilkes, H., & Kahmen, A. (2010). Leaf wax n-alkane δD values of field-grown barley reflect leaf water δD values at the time of leaf formation. *Geochimica et Cosmochimica Acta*, *74*(23), 6741–6750.